SANDIA REPORT
SAND2012-1447
Unlimited Release
Printed March 2012

Characterization of Hydraulic and Ignition Phenomena of Pressurized Water Reactor Fuel Assemblies: Phase II Test Plan

S.G. Durbin and E.R. Lindgren

Prepared by
Sandia National Laboratories
Albuquerque, New Mexico 87185 and Livermore, California 94550

Sandia National Laboratories is a multi-program laboratory managed and operated by Sandia Corporation, a wholly owned subsidiary of Lockheed Martin Corporation, for the U.S. Department of Energy's National Nuclear Security Administration under contract DE-AC04-94AL85000.

Issued by Sandia National Laboratories, operated for the United States Department of Energy by Sandia Corporation.

Available to DOE and DOE contractors from
U.S. Department of Energy
Office of Scientific and Technical Information
P.O. Box 62
Oak Ridge, TN 37831

Telephone: (865) 576-8401
Facsimile: (865) 576-5728
E-Mail: reports@adonis.osti.gov
Online ordering: http://www.osti.gov/bridge

Available to the public from
U.S. Department of Commerce
National Technical Information Service
5285 Port Royal Rd.
Springfield, VA 22161

Telephone: (800) 553-6847
Facsimile: (703) 605-6900
E-Mail: orders@ntis.fedworld.gov
Online order: http://www.ntis.gov/help/order-methods/#online

SAND2012-1447
Printed March 2012

Characterization of Hydraulic and Ignition Phenomena of Pressurized Water Reactor Fuel Assemblies: Phase II Test Plan

S.G. Durbin and E.R. Lindgren
Advanced Nuclear Fuel Cycle Technologies

Sandia National Laboratories
P.O. Box 5800
Albuquerque, New Mexico 87185-MS0537

Abstract

This report summarizes the strategy and preparations for the second phase in the Sandia Fuel Project (SFP) test program. During this phase, five full-length, prototypic 17×17 PWR fuel assembly will simulate a severe loss-of-coolant-accident in the spent fuel pool whereby the fuel is completely uncovered and heats up until ignition of the cladding occurs. Electrically resistive heaters with Zircaloy cladding will substitute for the spent nuclear fuel in the center assembly. This heated assembly will be placed in the center cell of a 3×3 pool rack and will be surrounded by four unheated mock fuel bundles. This arrangement will imitate the situation of a recently offloaded assembly surrounded by much older and thus lower decay heat assemblies.

The designs and plans detailed in this report are based on previous testing efforts and represent the current knowledge base. However, these results are subject to change with new information.

This page intentionally blank

TABLE OF CONTENTS

FIGURES

TABLES

ABBREVIATIONS/DEFINITIONS

BWR	boiling water reactor
CFD	computational fluid dynamics
CYBL	cylindrical boiling
DAQ	data acquisition
D_H	hydraulic diameter
ID	inside diameter
LDA	laser Doppler anemometer
MB	Management Board
MELCOR	severe accident analysis code
NEA	Nuclear Energy Agency
NRC	Nuclear Regulatory Commission
OD	outside diameter
OECD	Organization for Economic Co-operation and Development
PCT	peak cladding temperature
PRG	Program Review Group
PWR	pressurized water reactor
RGA	residual gas analyzer
SFP	spent fuel pool or Sandia Fuel Project
slpm	standard liters per minute (standard defined at 0ºC and 1 atm)
SNL	Sandia National Laboratories
TC	thermocouple

1 INTRODUCTION

1.1 Objective

The objective of the proposed project is to perform a highly detailed thermal-hydraulic characterization of full-length, commercial 17×17 pressurized water reactor (PWR) fuel assembly mock-ups to provide data for the direct validation of MELCOR or other appropriate severe accident codes. MELCOR model predictions based on extrapolations from the results of a previously conducted boiling water reactor (BWR) study indicate that PWR assemblies will ignite and radially propagate in a spent fuel pool complete-loss-of-coolant accident.[1] The proposed PWR characterization will be similar to that successfully conducted for the BWR study and will lead to a full-scale PWR fire test where the zirconium alloy cladding is heated in air to ignition. The PWR experimental design and data analysis will be closely coupled with MELCOR modeling as was done in the previous BWR study.

1.2 Testing Outline

As previously stated, the study will be conducted in two phases. Phase I of the test series has been successfully concluded as of this writing.[2] Phase II will focus on radial heating and burn propagation in five full-length assemblies. The fuel assemblies will be arranged in a pool rack with the heated assembly in the center cell. The four peripheral fuel assemblies will each share a cell wall with the center assembly and will be unheated, representing older spent fuel. All mock fuel assemblies will be constructed with zirconium alloy cladding and prototypic structural components. The center assembly will be constructed with electrically resistive heaters. The thermal mass of the compacted MgO powder used to make the electric heater is an excellent match to spent fuel as demonstrated in the previous BWR study. The peripheral assemblies will be loaded with MgO pellets in order to closely match the thermal mass of spent fuel. Two of the four peripheral assemblies will be pressurized with argon to simulate ballooning of the fuel clad during the ignition test. The baseline, testing parameters for Phase II are summarized below.

- One characteristic pool cell size – 224.5 mm nominal inner dimension for pre-ignition and ignition testing, respectively
- Pre-ignition test powers – 2 to 10 kW
- Ignition test power – 15 kW electrical input (Simulates approximately 16 weeks from offload)

The ignition test will determine the location in the center assembly where ignition first occurs and the nature of the burn propagation throughout the neighboring fuel assemblies. The unpowered peripheral assemblies will experimentally represent a “cold neighbor” situation and will demonstrate the potential of a locally initiated zirconium fire to spread through the remainder of a fully populated pool. The remainder of this report outlines the details of the Phase II test efforts. Note: The designs contained in this report are preliminary and are subject to refinement.

This page intentionally blank

2 APPARATUS AND PROCEDURES

2.1 General Construction

The testing in the Sandia Fuel Project (SFP) Phase II will focus on the nature of the zirconium fire in the five full-length fuel bundles and specifically the propagation of the fire from the center to the peripheral bundles. The test assembly will prototypically represent five commercial 17×17 PWR fuel bundles. The various components comprising a typical 17×17 PWR assembly are illustrated in Figure 2.1. The main structural component of the assembly is the core skeleton, which consists of eleven spacers permanently attached to twenty-five guide tubes. The 264 fuel rods pass through the spacers and are held captive in the assembly by the top and bottom nozzles.

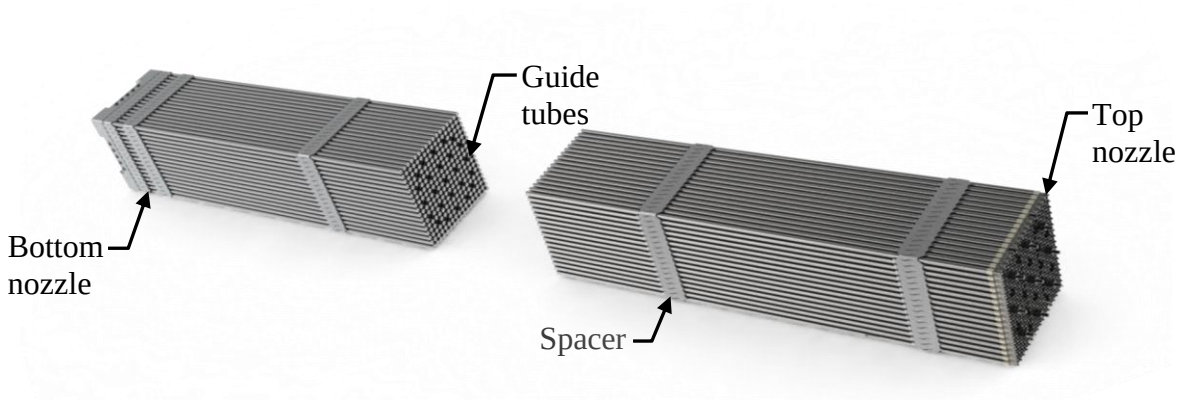

Figure 2.1 Various components in a typical 17×17 PWR fuel assembly.

The center heated PWR assembly will be fabricated using prototypic, commercial 17×17 PWR components and 9.53 mm (0.375 in.) heater rods made from 11.18 mm (0.44 in.) zirconium alloy tubing supplied by an industrial vendor. The wall thickness of the Zircaloy-2 cladding is approximately 0.71 mm (0.028 in.). The heater rods will be manufactured by a commercial vendor using the same fuel rod simulator design that was highly successful in the BWR study.[1] The spent fuel rod simulators for Phase II will have a linear power profile and a maximum output of 31.1 W/m (9.5 W/ft), which is twice that expected to produce ignition.

An important attribute of the mock fuel designs is the fact that the thermal mass of the magnesium oxide (MgO) powder used to simulate the spent fuel is virtually the same as spent fuel over the entire temperature range of interest (as shown in Figure 2.2). These spent fuel simulators will therefore heat at approximately the same rate and store the same amount of thermal energy as prototypic spent fuel rods. The magnesium oxide in the heated rods is constructed by compacting MgO powder around a coil of electrically resistive Nichrome wire. This compacted ceramic powder also forms the electrical insulation between the central heating element and the Zircaloy-2 cladding. The peripheral assemblies are constructed using sintered MgO pellets, which are inserted into Zircaloy-4 cladding. The distinction between the two types of mock spent fuel are due to differences in the as-built densities of the MgO inside the rods. The symbols in the plot for the Phase II heater and peripheral rods represent the measured, average value for each design.

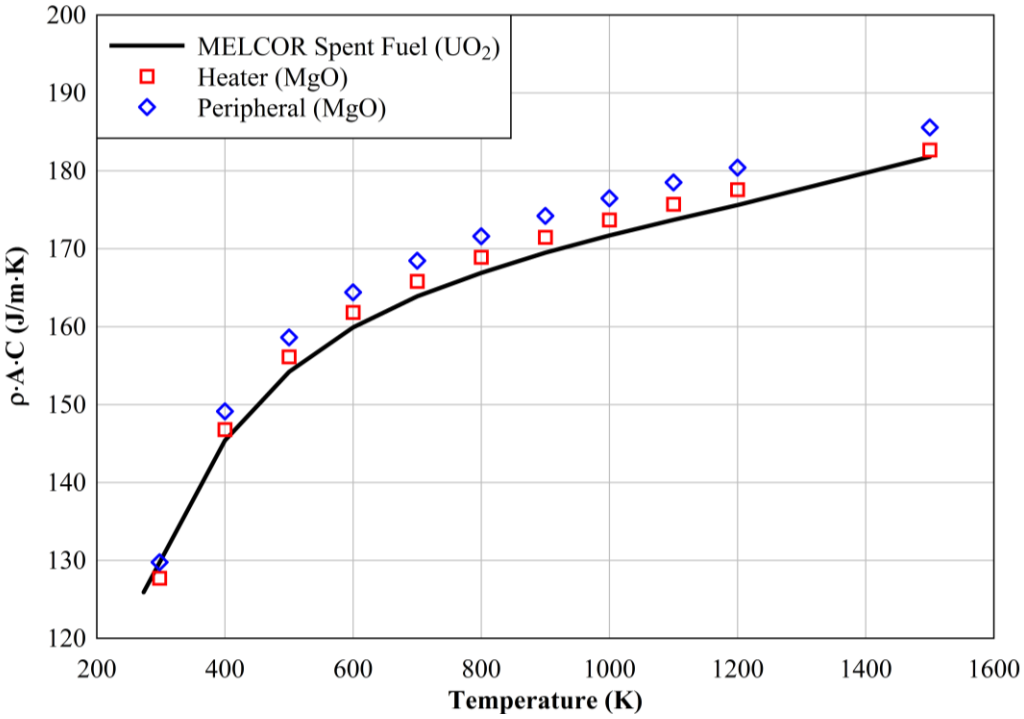

Figure 2.2 Thermal mass per unit length comparison of spent fuel and MgO fuel rod simulators.

Table 2.1 gives the individual and cumulative masses of all components within the SFP Phase II test assembly. Major sub-assemblies include the pool rack, PWR fuel skeletons, peripheral rods, and heater rods. The mass of thermocouples within the assembly is neglected.

Table 2.1 Masses of components in the SFP Phase II test assembly.

Part Name	Material	Quantity	Individual Part Weight (kg)	Total Part Weight (kg)
3×3 Pool Rack				
Tie bar	Stainless steel	32	0.04	1.31
Neutron absorber	Aluminum 1100	16	5.77	92.32
Internal sheathing	Stainless steel	16	6.70	107.19
Pool cell	Stainless steel	5	57.35	286.74
Shim stock	Stainless steel	8	0.87	6.93
Filler panel	Stainless steel	4	16.63	66.51
Subtotal				561.00
Skeleton				
Skeleton*	ZIRLO	1	32.67	32.67
Bottom nozzle	Stainless steel	1	5.26	5.26
Top nozzle	Stainless steel	1	5.71	5.71
Debris catcher	ZIRLO	1	1.43	1.43
Bottom bolts	Stainless steel	24	0.01	0.18
Guide tube inserts	Stainless steel	24	0.00	0.09
Subtotal				45.35
Peripheral Rods				
Cladding	Zr-4	1056	0.41	428.92
Top end plug	Zr-4	1056	0.003	3.33
Bottom end plug	Zr-4	1056	0.008	8.62
Plenum spring	Stainless steel	1056	0.01	6.29
MgO ceramic	MgO	1056	0.51	541.01
Subtotal				988.16
Heater Rods				
Cladding	Zr-2	264	0.54	142.20
MgO 142.25" heated + 2" unheated	MgO	264	0.50	133.18
MgO 10" upper unheated "plenum"	MgO	264	0.04	9.48
Subtotal				284.86
Phase II Assembly Total				1879.37

* Includes 24 guide tubes, 1 instrumentation tube, 7 full spacers, and 3 IFM spacers

2.1.1 Assembly Layout

Figure 2.3 shows the layout of the Phase II fuel bundles with and without the pool rack in place. The heated assembly is placed in the center pool cell and is surrounded by unheated assemblies. Two of these peripheral assemblies will be pressurized to simulate ballooning of the fuel cladding during the destructive, ignition test.

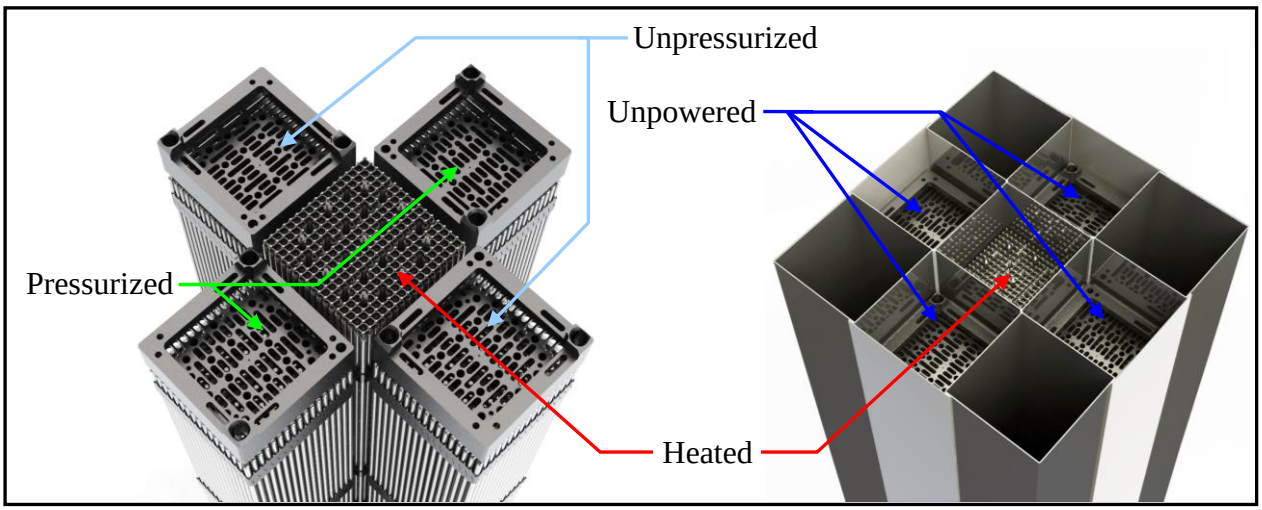

Figure 2.3 Layout of the Phase II test assembly.

2.1.2 Dimensions of the Test Assembly

The Holtec pool rack for Westinghouse 17×17 PWR assemblies incorporates pool cells with an inner dimension of 224.5 mm. Therefore, a 224.5 mm pool cell was the design basis for both the Phase I and Phase II ignition tests. As with the Phase I pool cells, the Phase II pool rack will be constructed of 1.91 mm (0.075 in.) thick stainless steel material. The actual inner dimensions of each of the pool cells are shown in Figure 2.4. The inner dimension of the center cell is nearly identical to the 224.5 mm design. The as-built peripheral cells are slightly smaller than the design with an average inner dimension of 222.7 mm, or less than a one percent difference. The insulation scheme for Phase II is also illustrated in Figure 2.4. The corner cells will be filled with high temperature insulation. The entire assembly will be surrounded by approximately 152.4 mm (6 in.) of the same high temperature insulation. A stainless steel thermal radiation barrier will be installed around the external insulation.

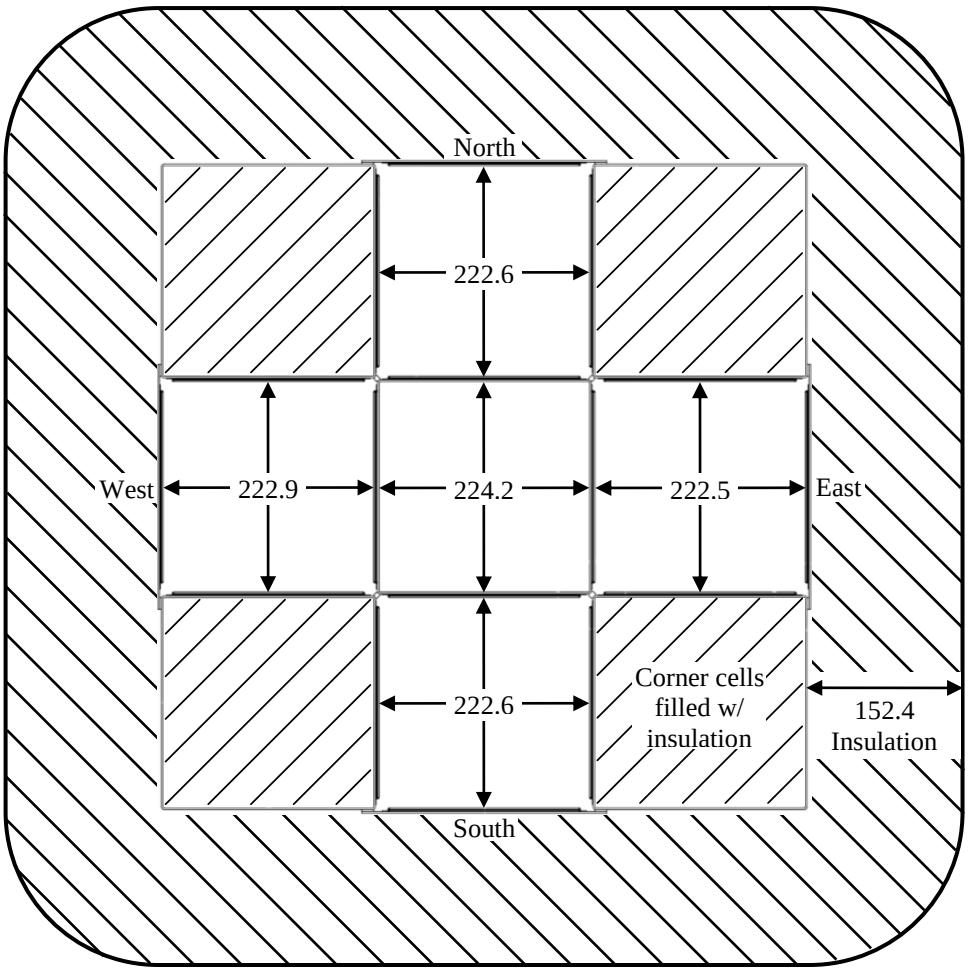

(All dimensions in mm)

Figure 2.4 Dimensions of the as-built pool rack and the design insulation thickness.

2.2 Design of the Heated Fuel Bundle

2.2.1 Heater Design

The design for the Phase II heater rods is shown in Figure 2.5. This design is identical to those used in Phase I except that linear power density has been doubled for Phase II. The heated and unheated lengths for the fuel rod simulator and a PWR fuel rod are compared for reference. As shown in Detail A, the lower, unheated length of the heater includes a steatite standoff for electrical isolation 15.9 mm (0.625 in.) and an internal power introduction length 50.8 mm (2 in.). The height of the axial heated zone with respect to the top of the bottom nozzle is preserved as closely as possible between the heater rod 3.680 m (144.875 in.) and the reference PWR fuel rod 3.863 m (145”). Due to the necessary electrical connection at the top, the heater rod design has been extended 0.066 m (2.60 in.) above the prototypic length. Details of the top and bottom electrical connections are given in Section 2.2.2.

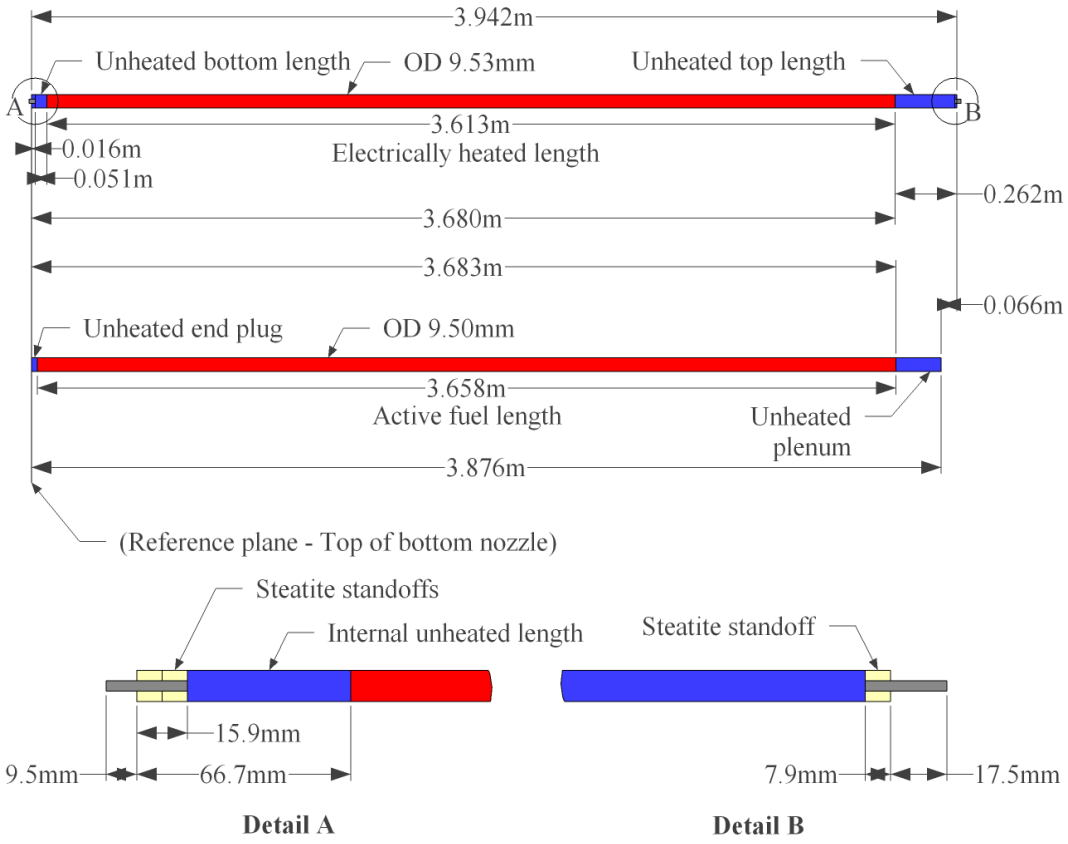

Figure 2.5 Design of the electrically heated fuel simulators.

The vertical dimension in the plan view has been scaled 6:1 to show the heated and unheated zones. PWR fuel layout shown for reference.

2.2.2 Heater Rod Electrical Connections

Introducing electrical power into the assembly presents several engineering challenges. An electrical current is fed into the assembly at the top of the assembly by applying voltage, up to 120 VAC, across the heater rods. The bottom electrical connections terminate in the bottom nozzle, which is tied to the circuit neutral leg. Electrically isolating the heater cladding, guide tubes, and pool cell are crucial to prevent a short circuit in the power loop. In addition, the top electrical connections are expected to reach highly elevated temperatures. Designs have been engineered to address these testing issues. This is the same design that was successfully fielded during Phase I testing.

The peak temperature at the top of the assembly prior to ignition is projected to be 1100K, which is 200 K higher than experienced in the BWR ignition tests. Therefore, the upper heater rod electrical connection requires special attention. The high upper temperatures could lead to loss of electrical connectivity prior to ignition. The upper electrical bus plate and connections are specifically designed to survive at higher temperatures. Figure 2.6 shows a rendering of the design of the top electrical bus plates. The bus plates are cut from three pairs of nickel-copper alloy 400 (Monel) plates and will replace the top nozzle. The bus plates are electrically divided into three zones of 88 heater rods each to accommodate the higher power requirements expected in the Phase II experiment and facilitate installation of the bus plates onto the heater rod power

posts. To insure even distribution of power to the heater rods, the power will be introduced into each zone via three 6.4 mm (0.25 in.) Monel threaded rods as shown in Figure 2.6.

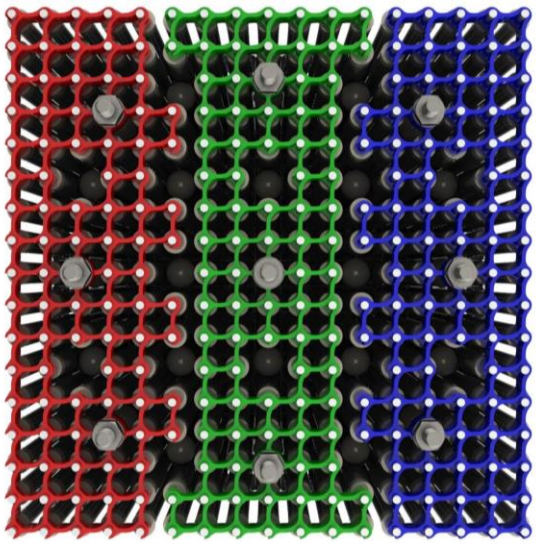

Figure 2.6 Design of the top electrical bus plate.

Each bus plate zone is comprised of a pair of upper and lower plates. The heater rod connection collars for the 88 heater rods are open on the same quadrant corner on a given plate. The connection collars on the mating plate are open on the opposite quadrant. When installed, the 88 heater rod connection pins initially pass through the plate in the larger interstitial area between four pin connection collars. Then, the plate is slid diagonally until all of the heater rod pins are captured in the connection collars. The top and bottom plates are moved in opposite directions so once in position each heater rod pin has 360° contact with the connection collar as shown in Figure 2.7. The Monel threaded rods are truncated in this rendering. For the actual installation, the all-thread rods extend approximately 1 m above the bus plates before transitioning to a traditional copper power lead.

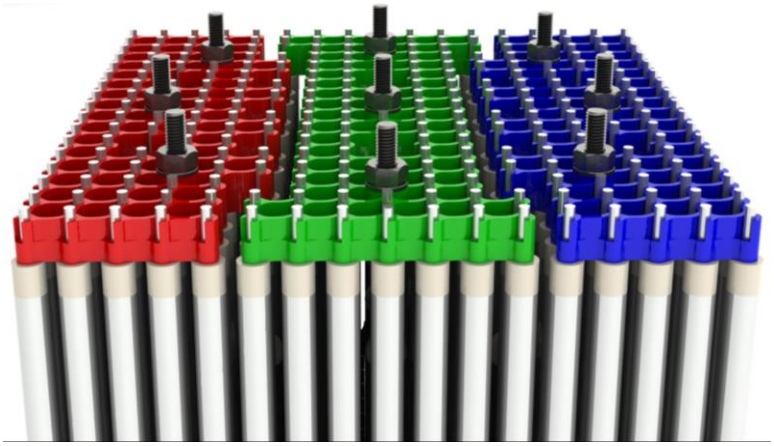

Figure 2.7 Assembly detail of the top electrical bus plate design.

The top of the assembly is represented schematically in Figure 2.8. The top electrical bus plates have been left out of the drawing to avoid confusion. Figure 2.8 shows the top of two heater

rods and a guide tube in cross section. Steatite standoffs and an alumina sphere isolate the cladding and guide tubes from electrical contact with the top bus plates. The additional length of the heater rods over the prototypical value is required to place the electrical connection above the top of the guide tubes. A detailed drawing of the power connection, including the top bus plates, is shown in Figure 2.9.

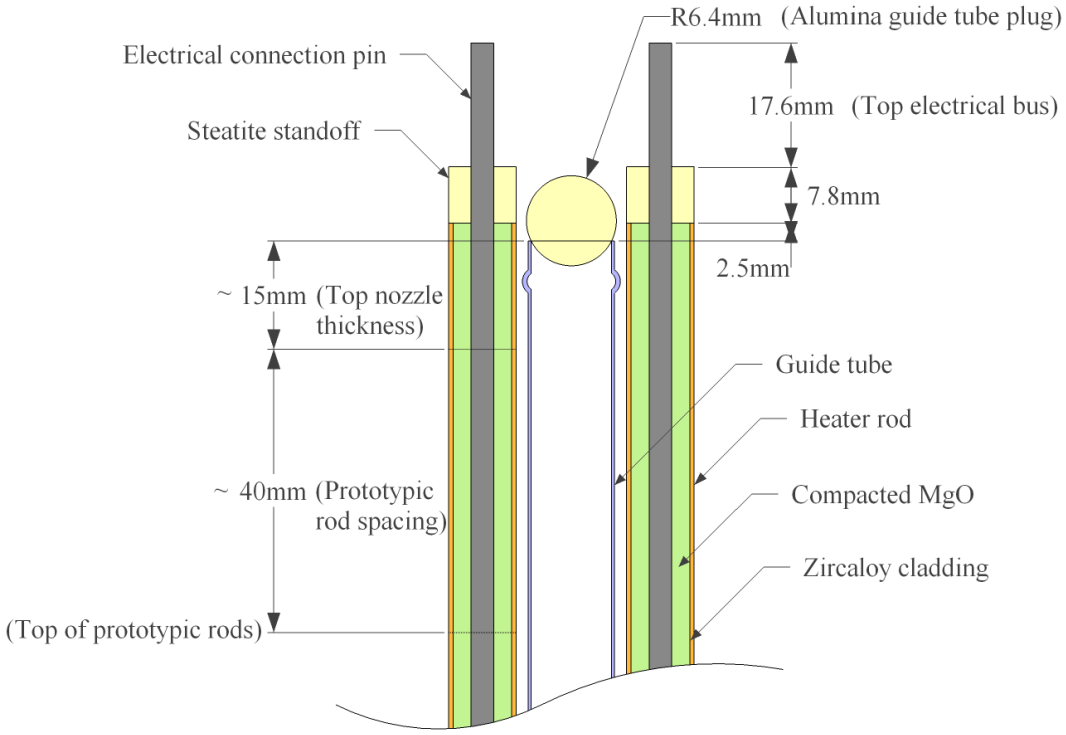

Figure 2.8 Detail drawing of the top of the assembly showing two heater rods and a single guide tube.

The top and bottom plates are held in place by the threaded Monel power rods as shown in Figure 2.9. On the lower plates, the power connection locations are threaded to receive the power rod. The power connection locations on the top plate are slightly oversized, through holes. The power rod is passed through the upper plate and threaded into the lower plate. A Monel nut and washer is tightened down onto the top plate to lock the plate together.

The bottom PWR nozzle will serve as the electrical bus for the neutral connections. Blind holes machined into the bottom nozzle will accept the connection pin of each heater rod as shown in Figure 2.10. High temperature silver contact grease will be placed in each hole to insure good connectivity.

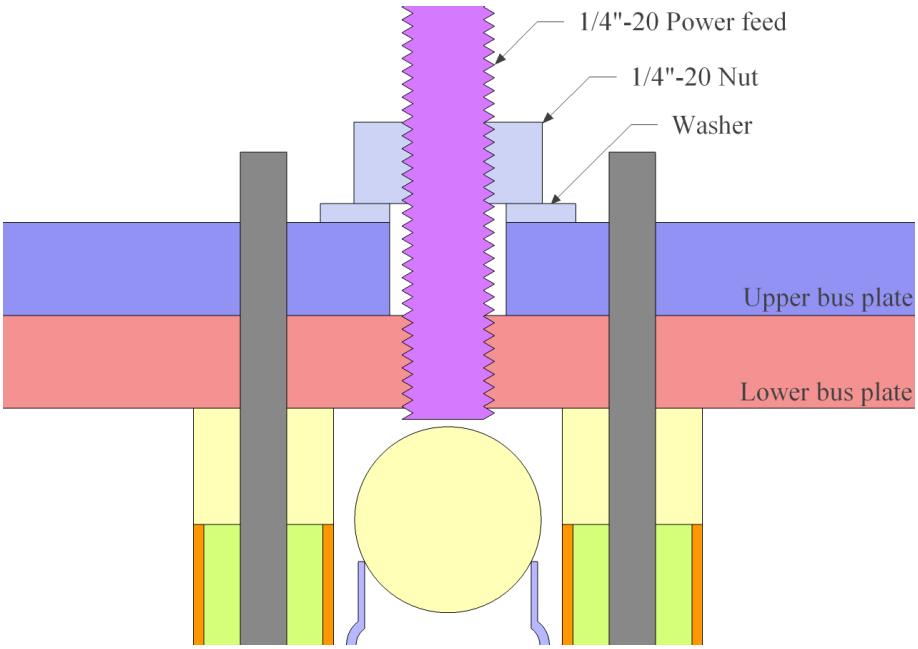

Figure 2.9 **Cross-sectional detail drawing of the top electrical connection from the power feed into the heater electrical pins.**

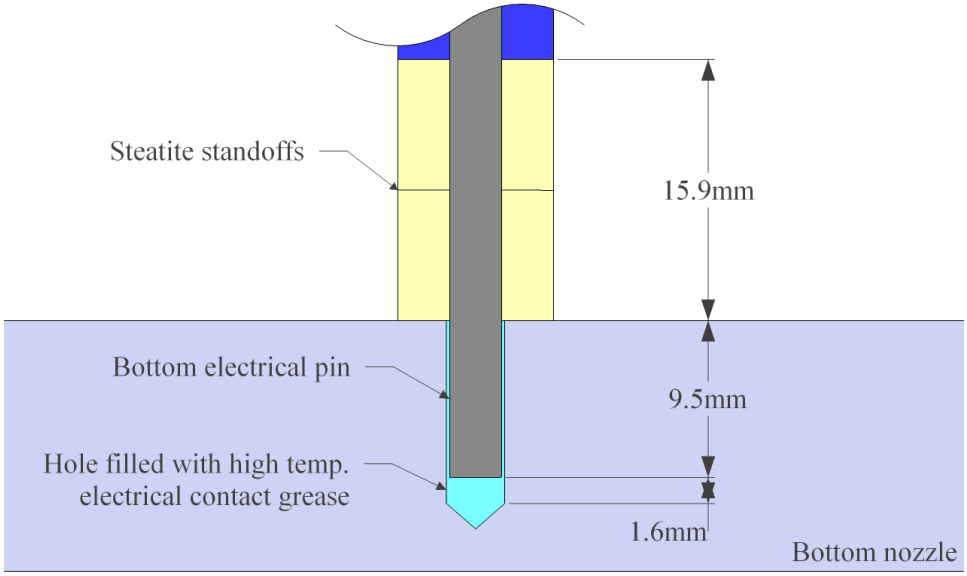

Figure 2.10 **Detail drawing of the bottom of the assembly showing the electrical connection of a single heater rod to the bottom nozzle (neutral).**

Figure 2.11 shows the configuration of the power control system for the SFP Phase I test series. The data acquisition (DAQ) system generates a power set point based on user input via a LabVIEW graphical user interface. This set point signal is relayed to a proportional-integral-derivative (PID) controller. The PID controller determines an appropriate power control signal by comparing the power set point to the feedback signal from the system Watt transducer. The silicon controlled rectifier (SCR) power controller receives the control signal and allows the prescribed electrical power into the resistive load of the test assembly.

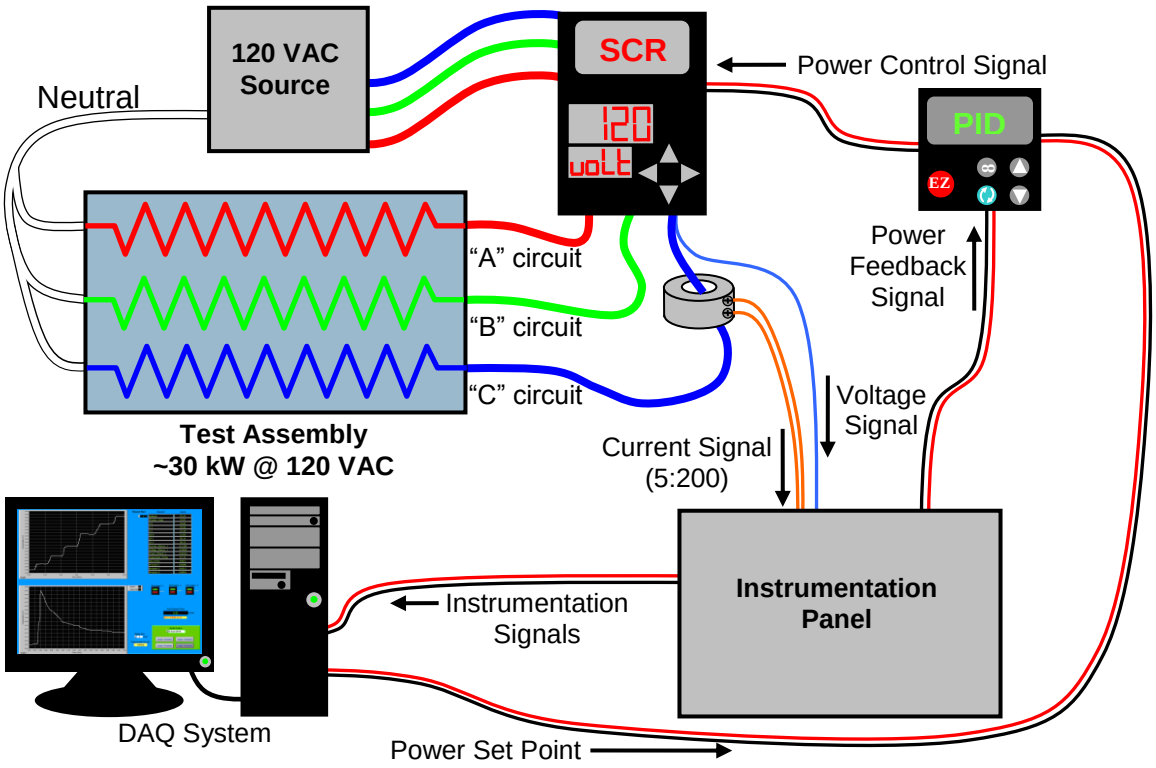

Figure 2.11 Power control system and test circuits.

Note: Power instrumentation and control shown only for "C" circuit. Actual installation includes instrumentation and PID control for all three circuits.

The internal layout of the instrumentation panel is shown in Figure 2.12. The transducers measure Watts, voltage, and current applied to the assembly. The signal from the Watt transducer is output to the DAQ and the PID controller as a feedback signal. The components used in this testing are listed in Table 2.2.

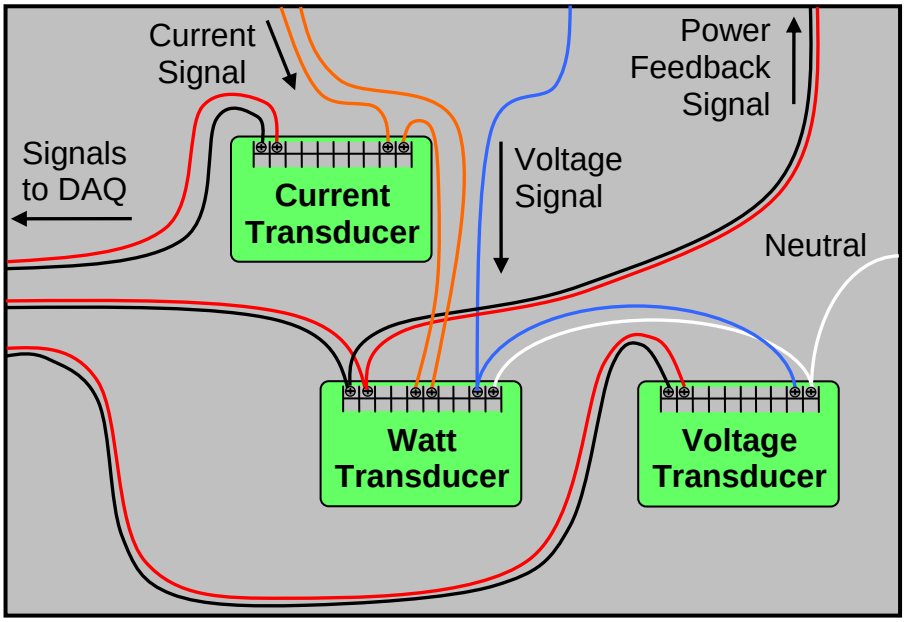

Figure 2.12 Schematic of the instrumentation panel for "C" circuit.

Table 2.2 List of equipment used for power control.

Description	Manufacturer	Model
AC Watt Transducer	Ohio Semitronics	PC5-001D
AC Voltage Transducer	Ohio Semitronics	3VTR-001D
AC Current Transducer	Ohio Semitronics	3CTR-010D
PID Controller	Watlow Electric Manufacturing	PM6C1FJ1RAAAAA
SCR Power Controller	Watlow Electric Manufacturing	PC91-F25A-1000

2.3 Instrumentation

The instrumentation of the prototypic PWR assembly will be similar to that used in the previous Phase I study. Five full-length PWR fuel bundles will be positioned inside a prototypic storage rack that is surrounded with a thick layer of high temperature insulation (see Figure 2.3 and Figure 2.4). The instrumentation will include hot wire anemometers, oxygen sensors, residual gas analyzer (RGA) for Ar and N_2 quantification, strain gauges, and thermocouples (TCs).

2.3.1 Center Bundle Thermocouples

A total of 163 TCs will be located within the center bundle. The TCs will be attached to the heaters and guide tubes by strapping the tip of the TCs with a small piece Nichrome shim stock to the rod. The shim stock is spot welded to the rod ensuring good thermal contact as shown in Figure 2.13. An additional piece of Nichrome was attached a short distance away from the tip of the TC to provide strain relief. All TCs to be used in this testing are ungrounded, K-type with a 0.813 mm (0.032 in.) Super Omegaclad XL sheath diameter. The majority of the TCs used were Omega Engineering part number TJ192-CAXL-032U-192-SMPW-M.

Thermocouples will be installed using US customary units. The data file headers and TC identifiers give positioning in inches, e.g. C_J-9_124 is installed in the center bundle on the

middle instrument tube at z = 3.150 m (124 in.). Ignition in the PWR is expected to occur near the top of the assembly. Therefore, most the bundle TCs will be routed out the bottom of the assembly. TCs located at or above z = 3.30 m (130 in.) will be routed out the top of the assembly.

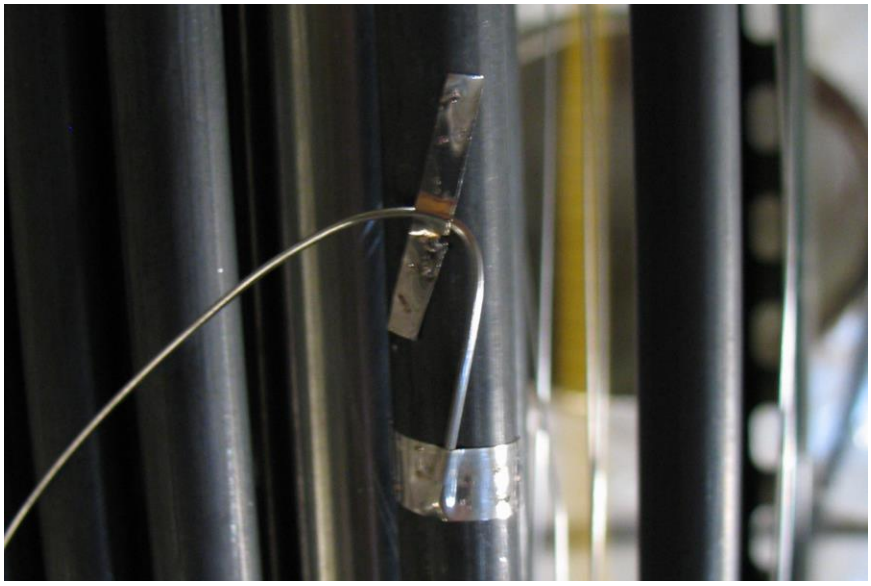

Figure 2.13 Detail view showing TC attachment to a fuel rod.

Figure 2.14 shows the TC layout of the center bundle. A majority of the TCs will be installed on the outside surface of the guide tubes before any of the heater rods are installed. TCs will also be installed on some outer row heater rods. Red denotes the location of high density arrays where TCs are located at 15.25 cm (6 in.) intervals. Yellow denotes the location of medium density arrays where TCs are located at 30.5 cm (12 in.) intervals. Green denotes the location of low density arrays where TCs are located at 61 cm (24 in.) intervals.

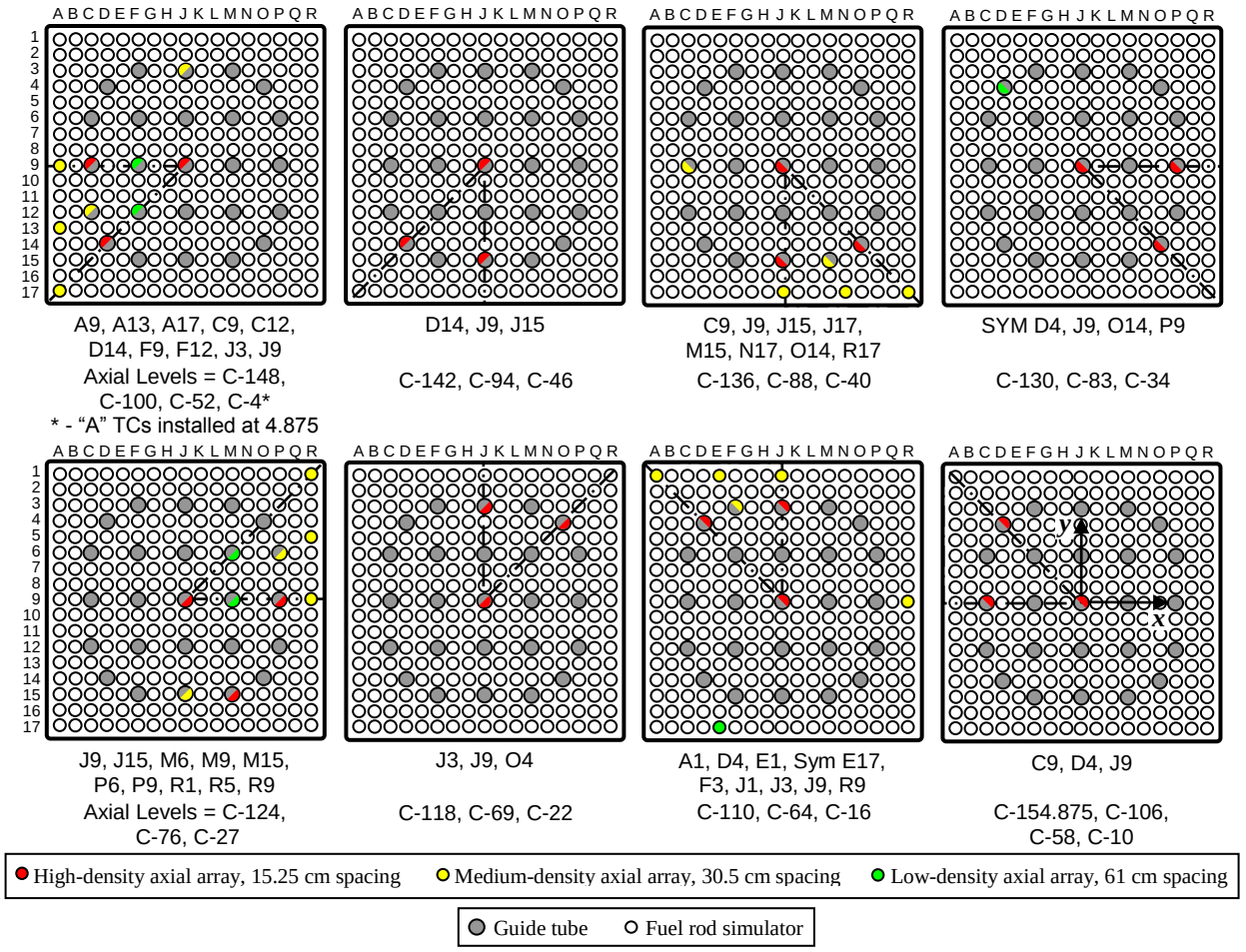

Figure 2.14 Thermocouple layout for the Phase II center, heated fuel bundle.

Note: The center bundle will be installed with rod A1 oriented nearest the Southwest corner of the center pool cell.

2.3.2 Peripheral Bundle Internal Instrumentation

Similar to the center assembly, the peripheral assemblies will be instrumented with TCs at 15.25 cm (6 in.) spacing. Unlike the center assembly, which is ideally symmetric about both the local *x*- and *y*-axes, the peripheral assemblies are symmetric only along the *x*-axis. Therefore the TCs are placed throughout these assemblies to measure the thermal gradient from the center-facing cell wall to the outer rack wall.

Figure 2.15 shows the layout of the thermocouples in the unpressurized, peripheral assemblies. An extra designator has been added to distinguish the global orientation of each bundle, e.g. "E" for East. An example TC designator is E_U_J-9_124 for a TC installed in the center of the East, unpressurized bundle at z = 3.150 m (124 in.).

Similarly, Figure 2.16 gives the layout of the internal instrumentation in the two pressurized, peripheral bundles. No TCs will be attached to the mock fuel pins because welding to the pressurized rods is prohibited. In addition to TCs, twenty-four strain gauges (Vishay Micro-Measurements Model CEA-03-062UQ-350) will be attached to the pressurized fuel pins as shown in the left diagram of Figure 2.16 in a 3-wire, quarter-bridge configuration. Twenty-three

of the gauges will be actively monitoring the strain in the cladding due to the internal pressure of the rods. These strain gauges are attached directly to the cladding in between the debris catcher elements between the z = 0.105 to 0.111 m (4.125 to 4.375 in.) levels. The remaining strain gauge will be attached to the nearby debris catcher as a control to quantify the apparent strain due to temperature changes experienced by the gauges.

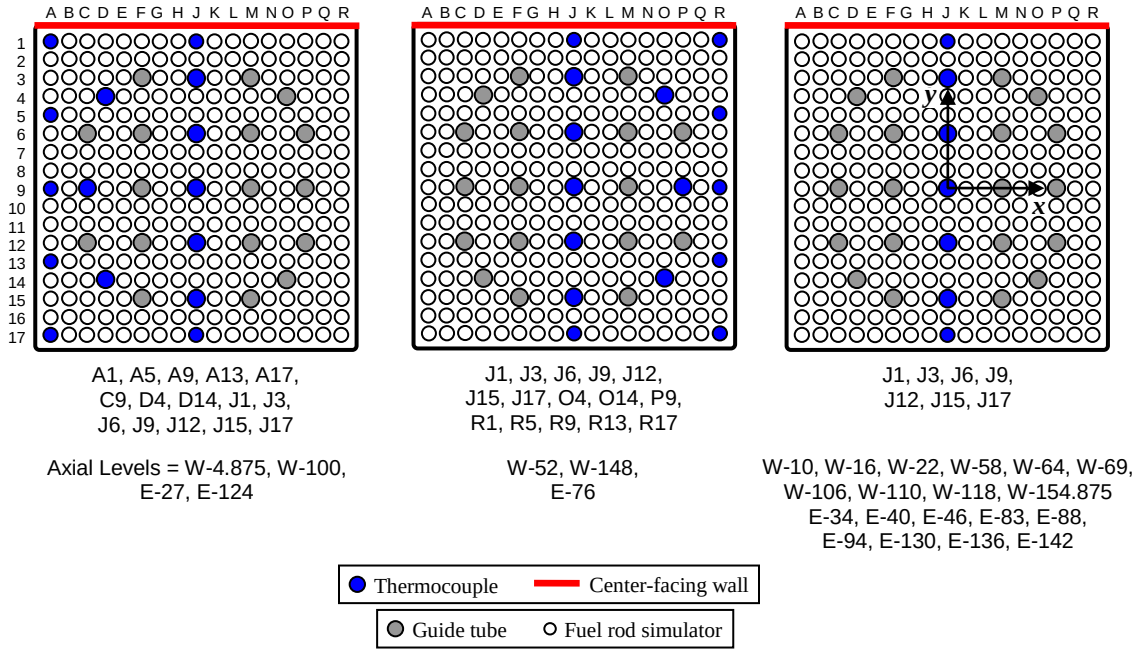

Figure 2.15 Layout of internal instrumentation for the unpressurized, peripheral fuel bundles.

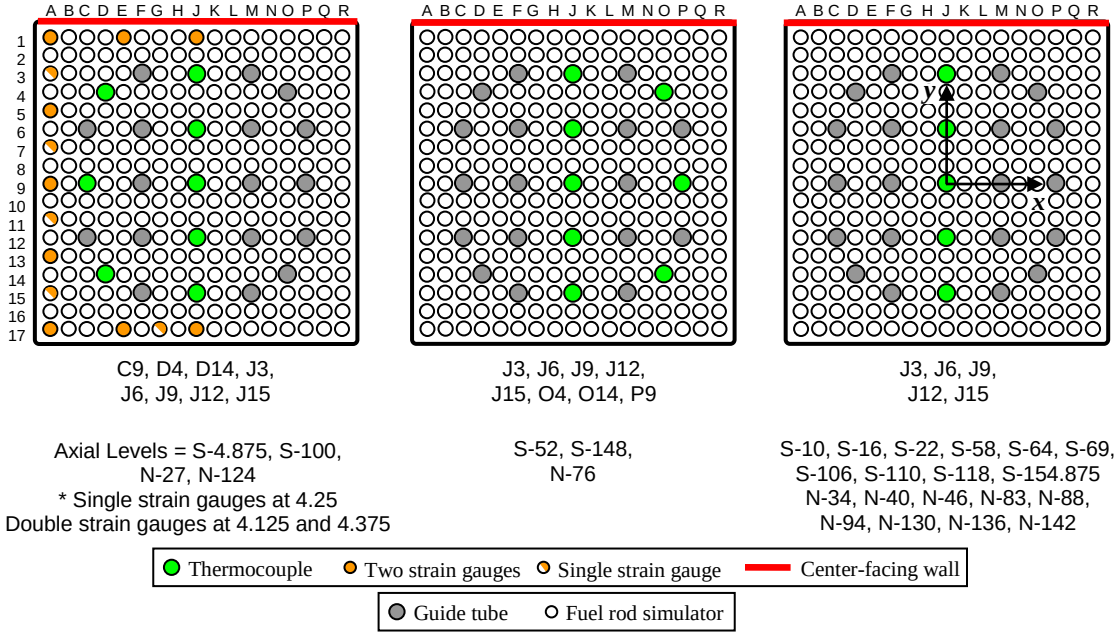

Figure 2.16 Layout of internal instrumentation for the pressurized, peripheral fuel bundles.

2.3.3 Other Thermocouples

A number of other TCs will be installed on the outer pool rack wall and on the outer stainless steel thermal radiation shield. These TCs will allow estimation of heat losses through the insulation. In addition TCs will be placed in the vessel at 0.61 m (24 in.) spacing from z = -1.22 to 5.49 m to measure ambient air temperatures around the test assembly.

2.3.4 Hot Wire Anemometers

Six hot wire anemometers will be placed in each of the 154 mm (6.065 in.) ID pipe that defines the inlet to the five test assemblies. One will be located in the inlet pipe of each of the peripheral assemblies and two will be located in the inlet pipe of the center assembly. Hot wire anemometers were chosen to measure the inlet flow rate because this type of instrument is sensitive and robust while introducing almost no unrecoverable pressure loss. A typical placement of the hot wire is shown in Figure 2.17. TSI Model 8455 hot wire anemometers will be used for these tests. A honeycomb element will be added to the inlet entrance to reduce the influence of any air flow disturbances within the experimental enclosure on the hot wire measurements. Also, the flow encounters a slight contraction of 127 mm (5 in.) as it passes from the inlet pipe through the base plate. This diameter of 127 mm was chosen based on commercial the designs of pool racks.

A series of unheated calibration runs will be performed to calibrate the output of the hot wire anemometer. With up to eight mass flow controllers (MKS Instruments Inc. Model 1559A), air flows will be metered into the bottom of each assembly via the inlet pipe, and the response of the anemometer will be recorded for each flow rate. A least-squares regression will be used to define the linear coefficients to convert the hot wire anemometer output to a volumetric flow rate during heated testing.

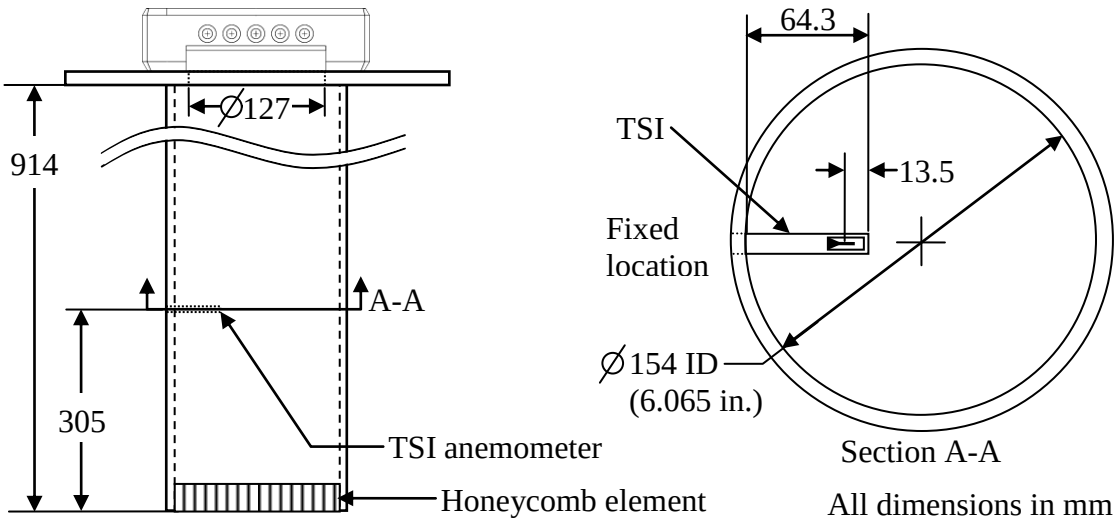

Figure 2.17 Positioning of the hot wire anemometers in the inlets to the fuel bundles.

2.3.5 Pressure Loss Measurements

A single pressure port will be installed near the top of the inlet pipe on each assembly to measure the isothermal pressure drop as a function of flow rate similar to previous efforts.[3] This data will

be used to determine the as-built, overall hydraulic loss coefficients of the apparatus. The pressure drop measurements will be made with a high precision quartz crystal differential pressure gauge (Parascientific Digiquartz Model 1000-3D) with a 0.02 N/m^2 (3E-6 psi) resolution.

The apparatus will be characterized in two distinct parts, the center assembly and the peripheral assemblies. The center assembly will be characterized separately much like in the Phase I testing. The four peripheral assemblies must be characterized as a group due to hydraulic communication (at the corners with the center cell) inherent in the prototypic pool rack. An equal flow will be simultaneously administered into each of the four peripheral assemblies with mass flow controllers and the overall pressure drop measured. The S_{LAM} and Σk for the four assembly ensemble will be determined from the quadratic fit of the pressure drop versus flow rate data similar to Durbin and Lindgren 2008.[3]

Additional geometric information of the center and peripheral fuel assemblies is provided in Appendix B. This information can used in conjunction with the information in Durbin and Lindgren 2008 for use in computational fluid dynamics (CFD) analyses.

2.3.6 Oxygen Sensors

Oxygen concentrations will be continuously monitored (Advanced Micro Instruments, Model 65, Part 6ANA0056) at six locations at the top of the assemblies as shown in Figure 2.18. The center assembly will be sampled at two locations, one near the center of the bundle (avoiding power leads) and the other from the annulus region between the power bus plate and the storage cell wall. Each of the four peripheral assembles will be sampled from the center of the bundle just above the top nozzle.

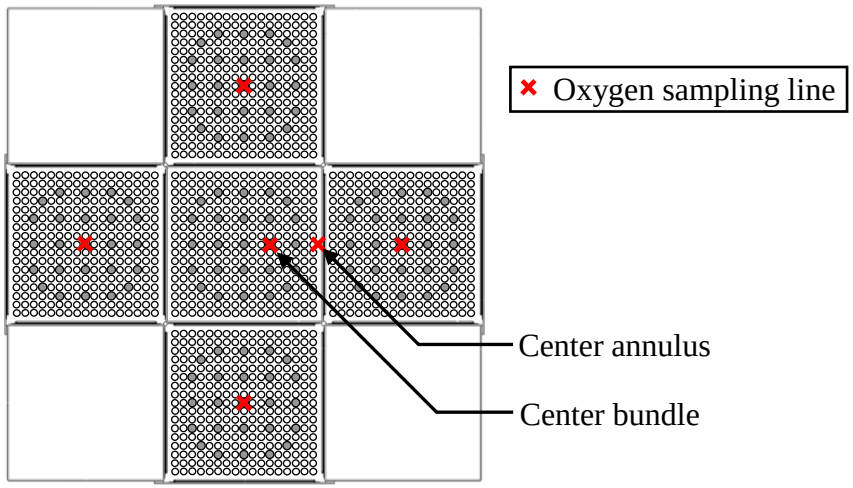

Figure 2.18 Schematic showing planned locations of oxygen sampling lines.

2.3.7 Residual Gas Analyzer

The nitrogen reactions within the burning center assembly will be monitored in order to determine the degree of zirconium nitride formation and eventual oxidation by Equations 2.1 and 2.2.

$$Zr + \tfrac{1}{2} N_2 \rightarrow ZrN \qquad \Delta H_{rxn} = -365.4 \text{ kJ/mol Zr} \qquad \textbf{2.1}$$

$$ZrN + O_2 \rightarrow ZrO_2 + \tfrac{1}{2} N_2 \qquad \Delta H_{rxn} = -729.4 \text{ kJ/mol Zr} \qquad \textbf{2.2}$$

Tracking nitrogen reactions will require simultaneous measurement of nitrogen and noble gas concentrations. The noble gases will behave as inert tracers. If nitrogen is consumed to form zirconium nitride, the ratio of nitrogen to the noble gases will decrease. When zirconium nitride is oxidized, nitrogen is released and the ratio of nitrogen to the noble gases will increase. The primary noble gas considered will be argon, but helium will also be monitored as a backup. The ballooning peripheral rods are pressurized with ultra-high purity argon so when the rods rupture the background concentration of argon in the CYBL vessel may be altered. As a mitigation, fresh air will be introduced at the bottom of the CYBL vessel and the top floor of the CYBL building will be actively ventilated. The total inventory of argon in the 528 pressurized rods is about half the amount of argon initially present in the air contained inside the CYBL vessel.

The amounts of nitrogen, oxygen, argon, and helium in the exhaust stream directly above the center assembly test bundle will be measured with a Pfeiffer RGA (Model GSD 300T). This instrument employs a heated quartz capillary for sampling air at ambient pressures (83 kPa). The instrument utilizes a tungsten filament for ionizing the sample and a quadrupole mass spectrometer for ion detection. A single ion (amu 28, 32, 40, and 4) will be used to monitor for each gas (nitrogen, oxygen, argon, and helium respectively). The data will be recorded every 10 seconds for the duration of the test. When significant oxygen is present in the sample before ignition, the detector current will be converted to a mole or volume fraction based on the analysis of ambient air. When oxygen is absent after ignition the detector output will be converted to mole or volume fraction based on the analysis of the five calibration gases described in Table 2.3. These calibration gases span nitrogen removal from 0 to 67% and nitrogen release from 0 to 67%. During the Phase I ignition test, nitrogen removal was found to range from 30 to 60%.

Table 2.3 List of proposed RGA calibration gases.

Calibration Gas	Ar (%)	He (%)	Balance N_2 (%)	N_2 / Ar	N_2 Removal (%)
1	3.54	0.0020	96.4	27	67
2	1.77	0.0010	98.2	55	34
3	1.18	0.0007	98.8	84	0
4	0.89	0.0005	99.1	112	-34
5	0.71	0.0004	99.3	140	-67

As in the Phase I ignition test, the RGA sample will be drawn from the sample stream used for the continuous oxygen monitor. This sample is collected through a ceramic tube near the center of the center assembly just above the bundle bus plate as depicted in Figure 2.18. The bus plate is located 0.173 m (6.82 in.) below the top of the storage cell. The sample for the RGA analysis will be filtered to remove particles that could plug the capillary inlet. The primary sample location will be from the bundle of the center assembly. However, valves will allow easy changeover to the annular sample location if needed.

2.4 Experimental Approach

The Phase II test matrix will be very similar to the corresponding Phase I test matrix . For the pre-ignition testing, the assembly will be heated at a given power and the resulting temperatures and induce flow rates determined. The peak temperatures must be kept below 900 K in order to

avoid excessive oxidation of the zirconium components. The cumulative temperature history of the zirconium components will be monitored and the resulting oxide layer produced will be estimated with MELCOR and used as an initial condition for the MELCOR modeling of the final ignition experiment.

The steady state buoyancy driven flow and resulting temperature profile are highly coupled. The thermal gradient inside the bundle creates the buoyancy that drives the flow. The flow in turn convectively cools the bundle such that the flow and the thermal gradients come into balance. The resulting data set provides an excellent validation database for any dynamic thermal-hydraulic numerical model of the assembly.

Once the experimental apparatus is constructed, hydraulic characterization will be performed as described above in Section 2.3.5. The hydraulic loss parameters determined from this characterization will be used in MELCOR modeling of the experimental apparatus.

Once all power, control, and data systems have been verified, pre-ignition testing will be conducted. Assuming that power scaling for the Phase II 1×4 assembly is similar to the Phase I assembly, the pre-ignition power will range from 2000 to 10000 W in 2000 W increments. Pre-ignition tests will be conducted for 12 hours or until 900 K temperature is reached anywhere in the apparatus. One low power test (e.g. 2000 W) will be repeated and conducted for 20 hours in an attempt to reach steady state.

The Phase II testing will conclude with a final, destructive ignition test. The required power for a 12 hour ignition is presently estimated to be approximately 15 kW. The cold neighbor boundary conditions experimentally represent 5+ year old neighbors.

3 DESIGN OF BALLOONING FUEL RODS

A significant technical challenge in Phase II of the Sandia Fuel Project (SFP) is the manufacture and installation of pressurized fuel simulators in two of four peripheral assemblies. Initial testing and evaluation of the welding techniques are required for the attachment of the prototypic end plugs to the rod cladding. After this qualification stage, 528 pressurized fuel rods will be manufactured for installation in two peripheral assemblies for Phase II pre-ignition and ignition testing. These efforts will incorporate prototypic test articles with Zircaloy-4 (Zr-4) cladding and end plugs.

An initial series of small-scale rodlets were produced to evaluate the acceptability of welds between the fuel end plugs and the cladding. Two types of welds were tested during this period. The first was an orbital weld between the cladding and the end plugs at both the top and bottom of the rodlet. The second was a closure weld in the top end plug to seal the rodlet. This closure weld fills a 0.64 mm (0.025 in.) through hole in the center of the top end plug. All welds used in this process are autogenous and are produced using tungsten inert gas (TIG) welding technology. These rodlets were then subjected to pressure leakage detection and heated ballooning experiments similar to those performed earlier in the SFP project to qualify weld integrity.

A production run of full-length rods will be commissioned upon decision of internal rod pressure. These rods will have magnesium oxide (MgO) pellets and a stainless steel spring installed inside of the cladding to simulate the thermal mass of spent nuclear fuel. Figure 3.1 compares the design of the Phase II peripheral rods with spent fuel. Due to a higher gas volume fraction in the simulated fuel region, the fill pressure of the Phase II peripheral rods will need to be compensated in order to mimic the pressure of spent fuel at the time of cladding rupture. The logic used to determine the fill pressures are discussed in more detail in this chapter.

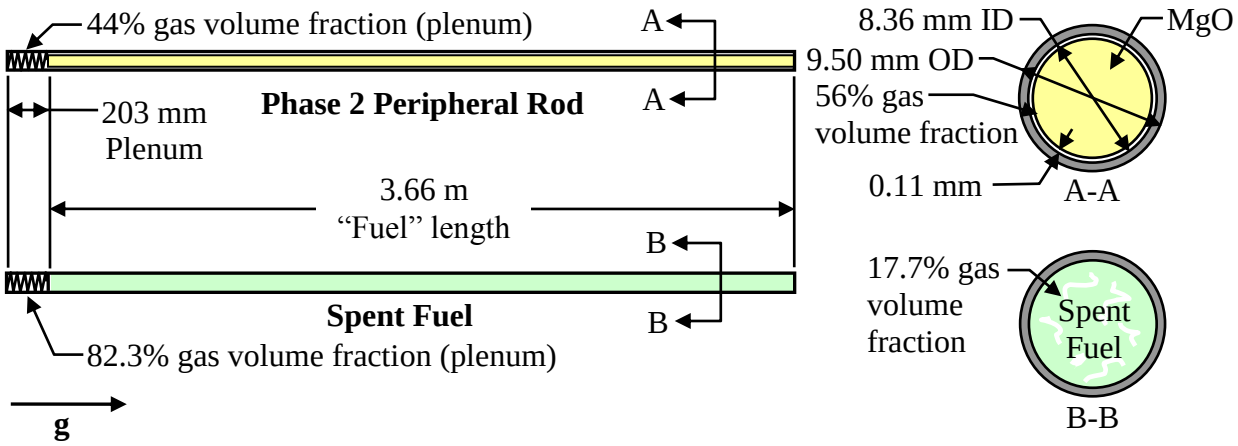

Figure 3.1 Schematic of the internal geometry of a Phase II peripheral rod and spent fuel.

3.1 Welding Techniques

3.1.1 Orbital Welds

Two orbital welds are required between the Zr-4 cladding and fuel end plugs, one at the top and another at the bottom of the fuel rod. Figure 3.2 shows a cross-sectional view of the setup for

welding the top end plug onto the Zr-4 fuel rod. Prior to the actual orbital welding procedure, both rod ends are reamed and parts thoroughly cleaned. External shield gas is provided by the orbital welding equipment.

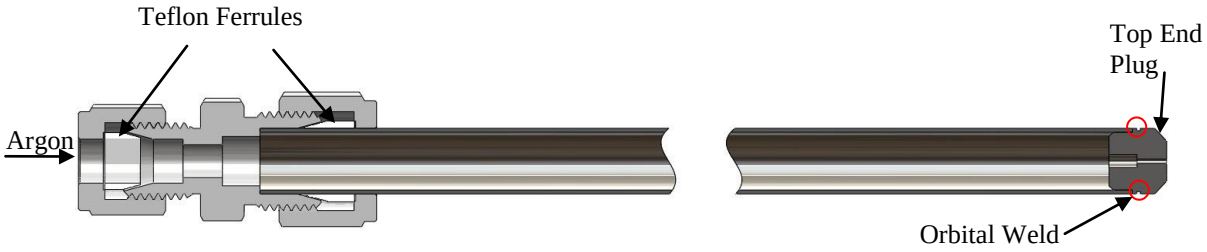

Figure 3.2 Top end plug weld setup.

With the top end plug welded, the argon purge setup is removed. The rod is then loaded with a stainless steel spring and MgO ceramic pellets as shown in Figure 3.3. Again, the design plenum spacing is 203.2 mm (8 in.).

Figure 3.3 Loading of fuel rod with MgO surrogate fuel and stainless steel plenum spring.

Figure 3.4 shows the reversal of purging system in which the top portion of the fuel rod is now inserted and secured into the purging apparatus. After purging the interior of the rod with argon, the bottom end plug is inserted and welded to the Zr-4 cladding. The Phase II peripheral fuel rod is now ready for final pressurization and closure welding.

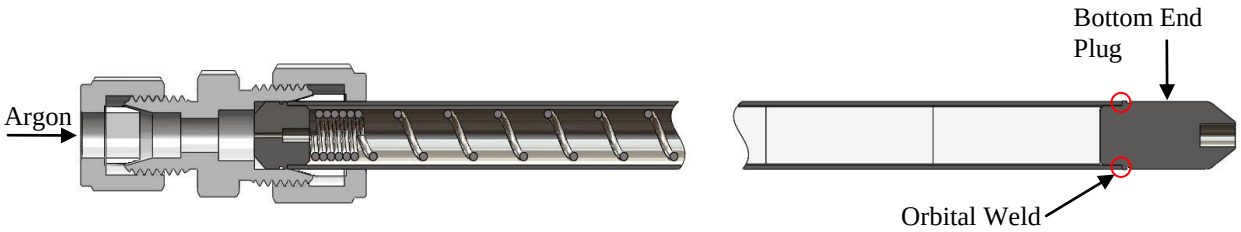

Figure 3.4 Bottom end plug weld setup.

3.1.2 Closure Weld

The 0.64 mm (0.025 in.) through hole in the top end plug is used to pressurize the rods and is then welded closed. Figure 3.5 shows the closure weld fixture (CWF). A TIG electrode is inserted and secured at a predetermined depth such that when the fuel rod is inserted a small gap exists between the electrode tip and top end plug surface. The assembled fuel rod is inserted until the chamfered portion of the top end plug is seated firmly against the chamfered opening of the hex bushing as shown in Figure 3.6.

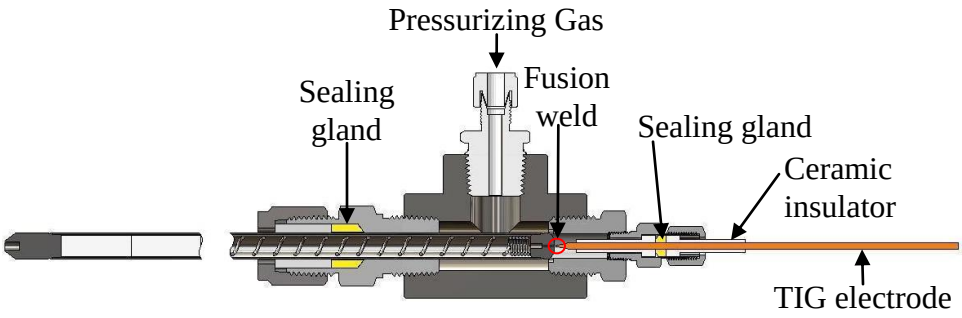

Figure 3.5 Schematic of the closure weld fixture.

Figure 3.6 shows a close up of the flow path of the fill gas. The hex bushing has two machined slots on opposite sides to accommodate gas flow. The hole in the top end plug provides the final opening for the pressurizing gas to pass through allowing purging and pressurization.

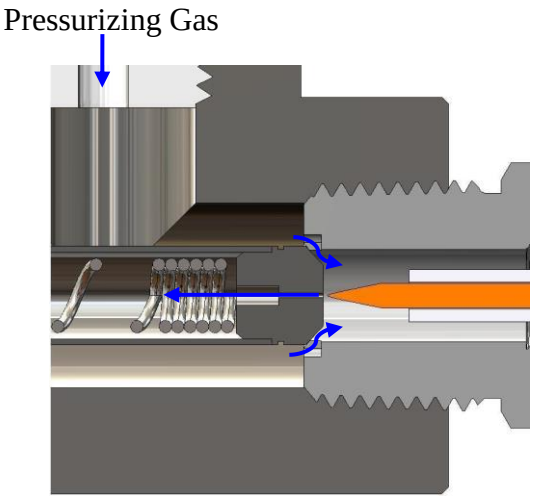

Figure 3.6 Close-up of gas fill process and top end plug weld location.

After all electrical connections have been configured, the final closure weld of the top end plug is made under pressure. Figure 3.7 shows a cross-sectional rendering and a photo of an actual welded top end plug. At this point the rod is fully pressurized and sealed.

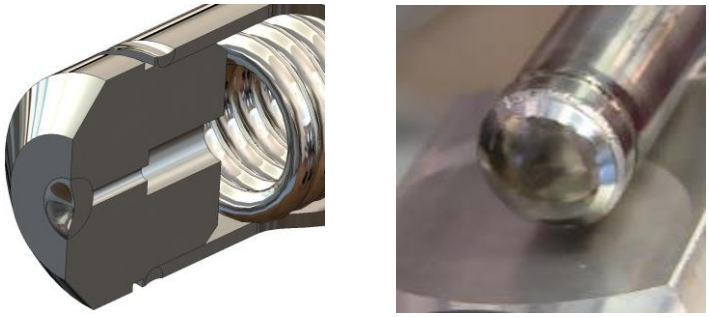

Figure 3.7 Top end plug closure weld.

3.2 Argon Fill Gas

Initial planning called for the use of helium to pressurize the Phase II rods. Initial attempts to implement a helium fill system for use with the SFP Phase II pressurized rods were unsuccessful in making the closure weld. Discussions with welding experts at Sandia National Laboratories (SNL) indicated that the high pressure helium gas is likely preventing sufficient ionization between the TIG welding tip and the top plug of the fuel element. For reference the first ionization energy of helium is approximately 1.6 times higher than argon. This ionization is crucial for forming and sustaining an electrical arc between the weld tip and the work piece. SNL was unable to determine from the fuel vendor their method of pressurization and closure. It is possible that the vendor utilizes some other technology such as laser or resistance welding that is not affected by the increased cover gas pressure.

As an alternative, argon will be used as a substitute gas. Successful welds under argon cover gas at pressures needed to simulate spent fuel have been demonstrated in repeatable fashion. Furthermore, the technical impact to the project is negligible. The thermal mass of argon in a pressurized rod is theoretically identical to that of a helium-filled rod. Although helium is almost one order higher with regards to thermal conductivity, the effect on the thermal response of the Phase II pressurized rods, which is on the order of seconds or less, is negligible considering the planned time scale of heated testing is on the order of hours.

Three ballooning tests have been conducted in final preparation for Phase II. The first two tests were conducted with a helium fill at pressures required to simulate the stress at rupture for spent fuel. These early tests had a compression cross-fitting near the bottom of the rodlet. This allowed the closure weld to be made before final pressurization. This compression fitting is not prototypic and is not compatible with the Phase II assembly. Figure 3.8 shows the layout of this rodlet. An 8 in. plenum was left at the top of the rodlet with the remainder of the cladding filled with Phase 2 MgO ceramic pellets (shown in the cutaway as yellow). Test 1 and 2 were conducted identically except that the Test 2 rodlet was shifted down in the tube furnace by 50.8 mm (2 in.) This shift was made to subject the closure weld to a higher temperature than expected in Phase II and therefore increase confidence in the survivability of the closure weld. All rodlets were centered inside an alumina process tube inside a tube furnace. The top end of the rodlets was unconstrained.

The Test 3 rodlet was made as a truncated version of the Phase 2 rods. A stainless steel tube with the same mass as the prototypic spring was substituted. Figure 3.9 shows the schematic of the Test 3 rodlet. Note the absence of the compression cross-fitting.

Finally, the top 12 in. of the three ballooning tests are shown in Figure 3.10. Again, Tests 1 and 2 were conducted with helium. Test 3 was filled with argon with a pressure to induce the same yield conditions as in Tests 1 and 2. The ballooning region in Test 2 is shifted by approximately 2 in. due to the unique placement of the article during this test as described earlier. All three tests demonstrate nearly identical ballooning, rupture, and buckling effects. No significant difference between helium and argon fills has been observed in ballooning tests.

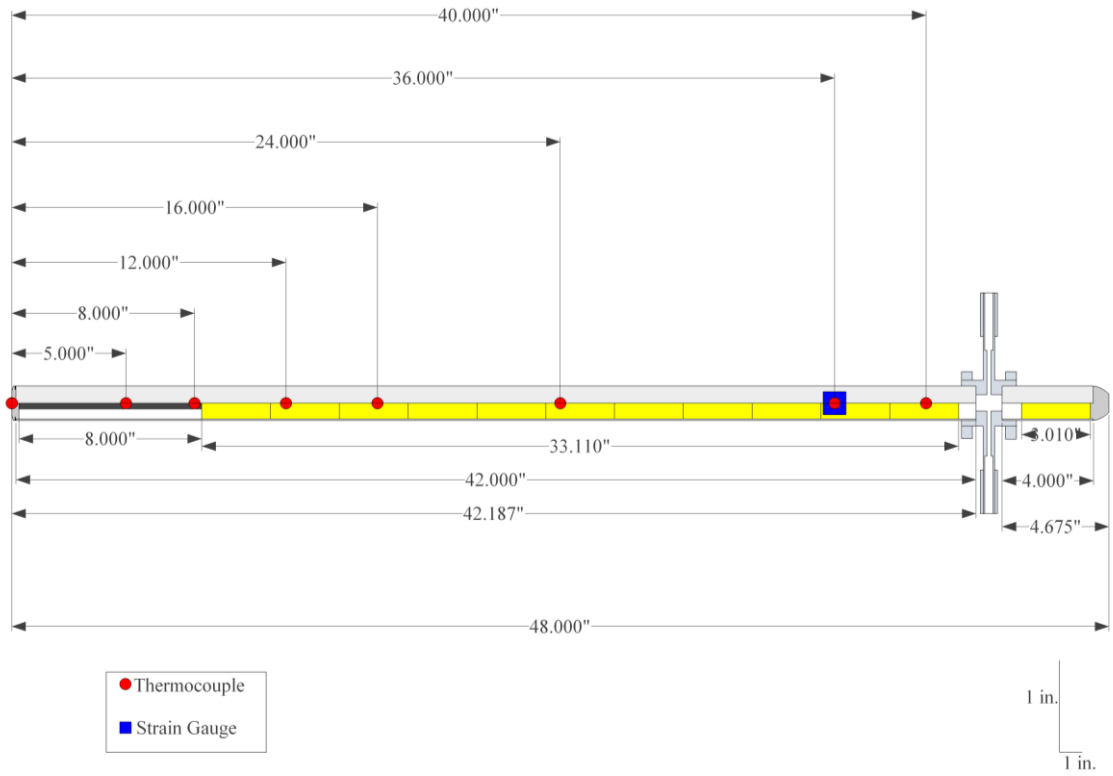

Figure 3.8 Schematic of the setup for rodlet ballooning Tests 1 and 2.

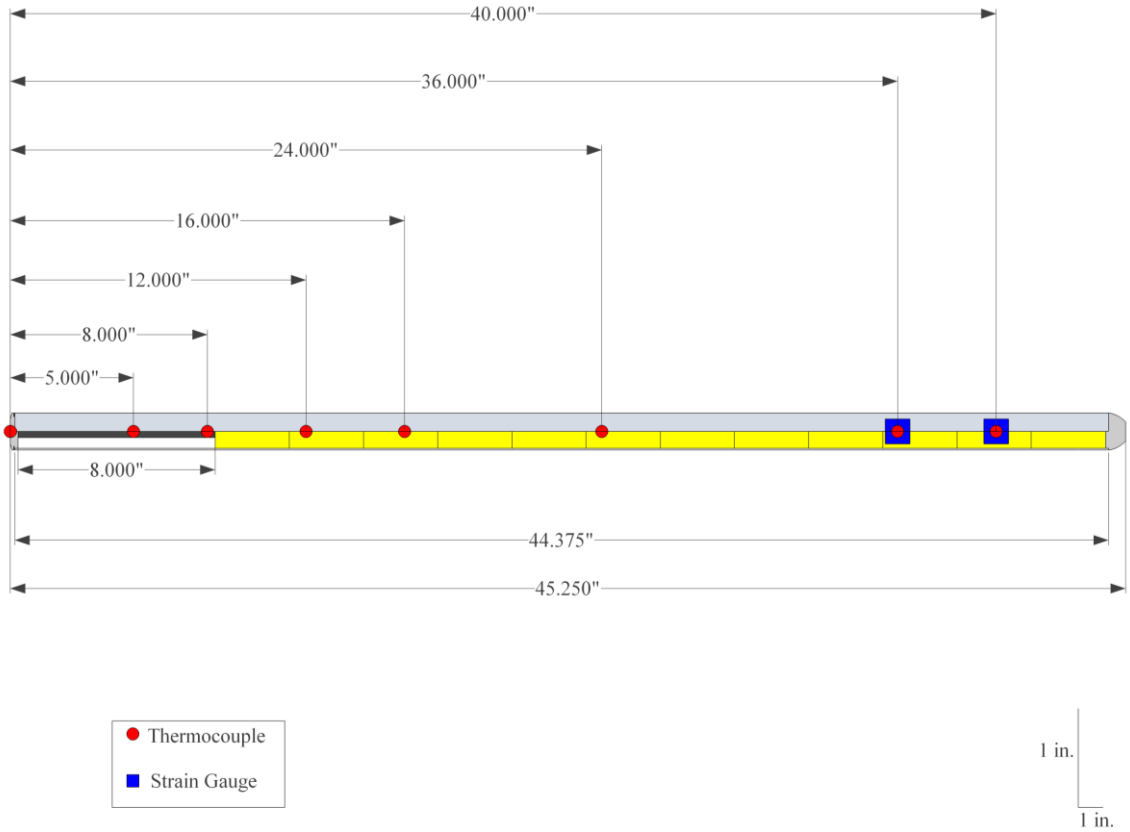

Figure 3.9 Schematic of the setup for rodlet ballooning Test 3.

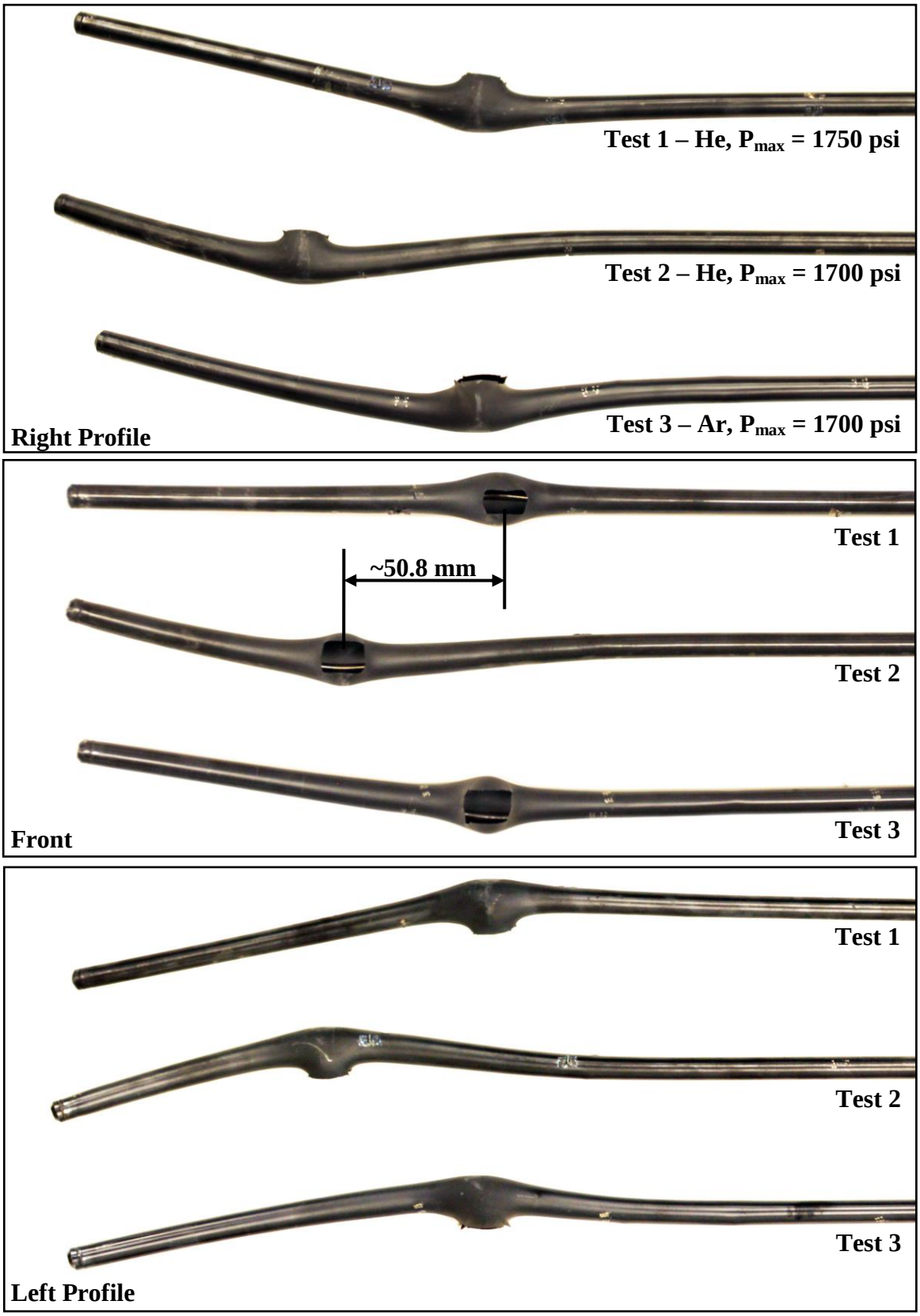

Figure 3.10 Photographs of the three ballooning rodlet tests.

3.3 Design Pressure(s) for Phase II Testing

A baseline, initial charging pressure of 5.2 MPa (750 psi) is recommended for the mock fuel in the SFP Phase II pressurized assemblies. This value translates to a predicted peak internal pressure of approximately 12 MPa (1740 psi) prior to ballooning. This peak pressure lies within the range of expected peak pressures typical of spent fuel in industry under similar accident conditions. Alternately, an initial charging pressure of 6.2 MPa (900 psi) would be required to simulate the upper end of the range for spent fuel. This design pressure would result in a peak internal pressure of 14 MPa (2030 psi) prior to ballooning.

Two options are being considered for Phase II of the SFP.

- Option 1 – Both assemblies initially charged to 5.2 MPa
- Option 2 – First assembly charged to 5.2 MPa, Second assembly charged to 6.2 MPa

The second option allows for the initiation of ballooning during two different time spans in the ignition test. However, having the two assemblies balloon at different times during the test could impose a significant asymmetry within the apparatus. At the time of the writing of this document, Option 2 is favored by a majority of the OECD partners, but a final vote has been deferred until the Program Review Group meeting.

3.3.1 Analysis of Fuel Rod Ballooning

Figure 3.11 summarizes the current strategy for pressurizing the SFP Phase II peripheral, mock fuel assemblies. This figure shows the pressure of different fuel designs as a function of peak cladding temperature (PCT). All calculations assume the ideal gas law and a 203.2 mm (8 in.) plenum. Note that the models used to determine the pressure response of the spent fuel and Phase II fuel rods do not simulate the plastic deformation incurred during ballooning. Therefore, these curves do not exhibit a peak pressure near the yield curve followed by depressurization at elevated temperatures. The compressibility of argon over the range of temperatures and pressures shown for the Phase II – P_o = 6.2 MPa curve is 0.98 to 1.04.

The black curve represents the equivalent pressure at yield for the 9.5 mm (0.374 in.) OD, 0.57 mm (0.0225 in.) thick Zr-4 tubing. The two dashed curves give the behavior of spent fuel undergoing the same heat up as expected during the Phase II ignition test. The two curves with triangles give the pressure response of Phase II rods at the two different initial pressures of 5.2 MPa (750 psi) and 6.2 MPa (900 psi). These pressures were chosen to cross the yield curve at approximately the same temperature and pressure as the average and upper values of spent fuel. Finally, the two solid lines with circular symbols show the measured pressure response of two design tests conducted in 2011. The pressure response of the Test 1 rodlet is flatter as a function of temperature because a more significant amount of the pressurizing gas is outside the heated zone. The pressure in Test 3 was determined solely from strain gauges, which began reading lower than expected for PCT > 700 K. The cause of this behavior was not determined.

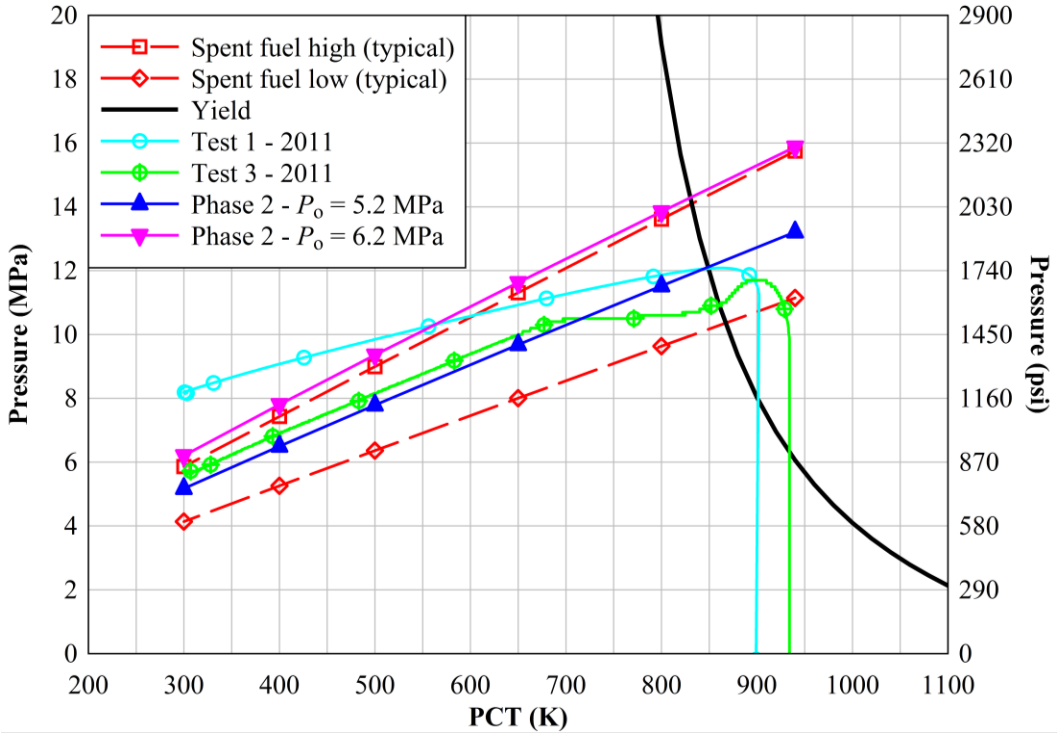

Figure 3.11 Pressure as a function of peak cladding temperature for different fuel designs of interest to the SFP Phase 2 test.

Figure 3.12 shows the temperature profiles along the length of the Phase II and spent fuel analytical models used to determine the pressure responses in Figure 3.11. These profiles were derived from Phase I test data. These temperature profiles include a greater amount of radial heat transfer than was encountered during the late stages of the Phase I test, PCT > 700 K. All the profiles were scaled from the average temperature profile in the assembly when the PCT was 650 K. Alternative temperature profiles (not shown) have been applied to the Phase II and spent fuel analytical models to determine the sensitivity of the pressure response. The Phase II rod and spent fuel models responded almost identically to each other as a result of the alternative temperature profiles. The equivalence of the pressure responses between the two designs increases confidence that the Phase II ballooning assemblies will respond similarly to spent fuel regardless of the actual temperature profile during the ignition test.

Figure 3.13 shows the temperature profiles used with the rodlet design analytical models. These profiles were derived from the first two design tests. As referred to in the discussion of Figure 3.11, a significant amount of the gas for the Test 1 rodlet was located outside the heated zone of the tube furnace. The initial pressure in this rodlet needed to be greater in order to achieve the pressure and temperature at yield associated with spent fuel.

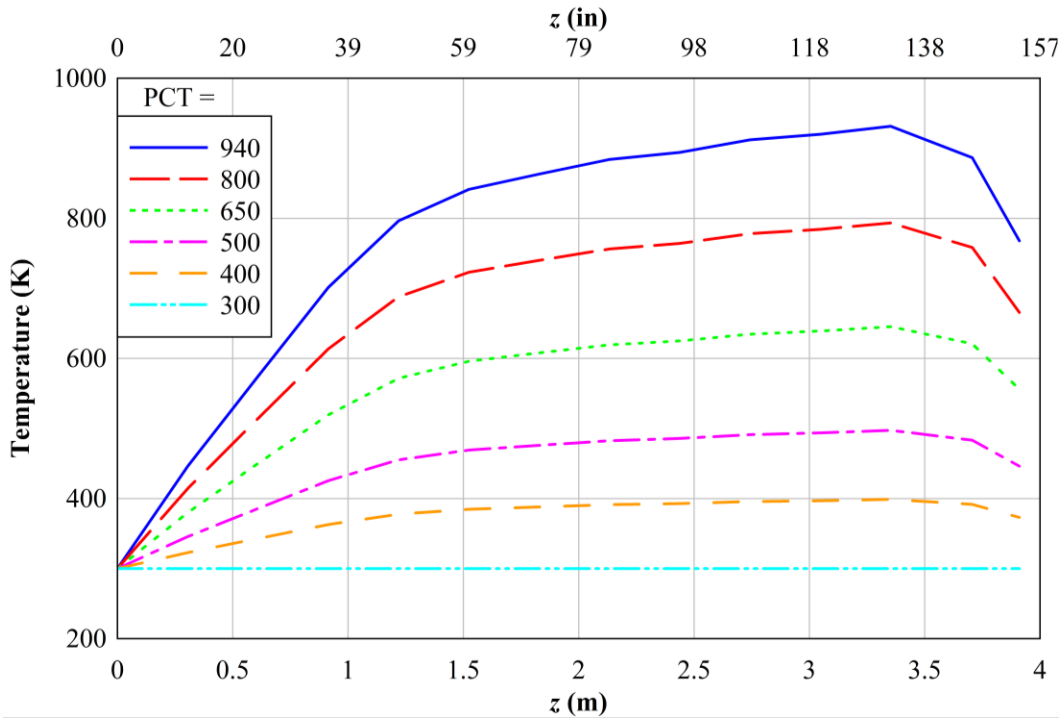

Figure 3.12 Temperature profiles for use with the Phase 2 and spent fuel analytical models.

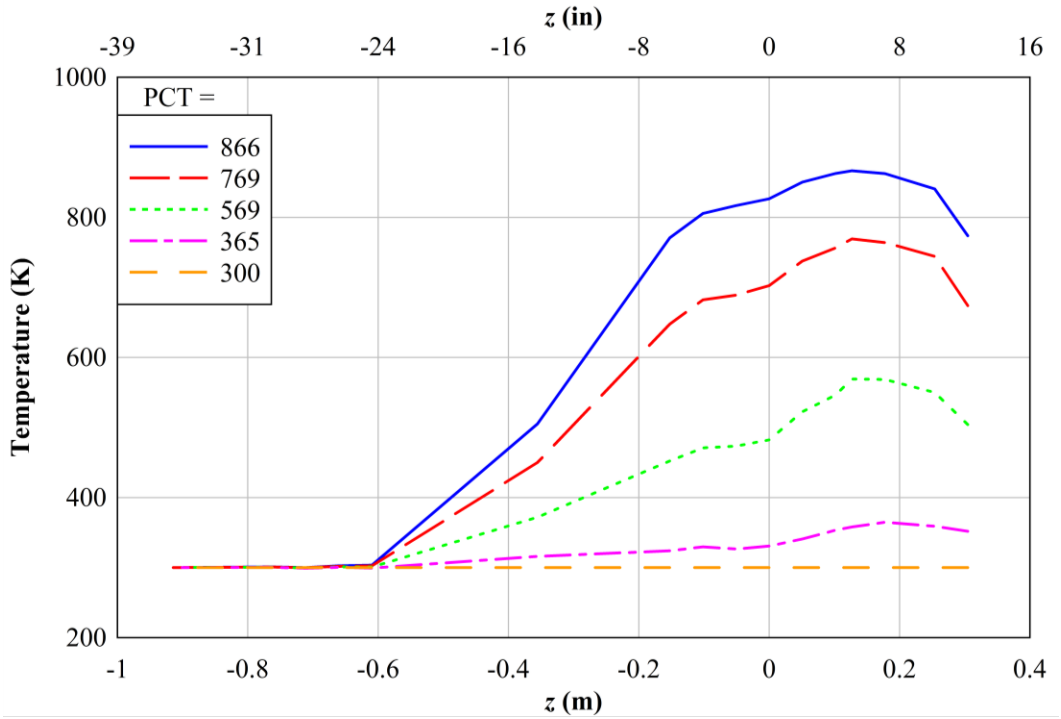

Figure 3.13 Temperature profiles for use with rodlet design analytical models.

This page intentionally blank

4 PROJECT STATUS AND SCHEDULE

Construction and procurement activities are proceeding to schedule. As of this writing, the first unpressurized, peripheral fuel bundle has been fully constructed and installed on the test stand. The center, heated assembly is approximately 90% completed. Final construction on the center assembly is expected to be complete by the end of this calendar year upon receipt of the final installment of heaters. The first pressurized, peripheral assembly is nearing 20% completion of thermocouple installation. A full complement of 264 rods have already been pressurized to 5.2 MPa (750 psi) for populating this assembly. In addition, Sandia National Laboratories (SNL) has loaded and prepared enough peripheral fuel simulators to complete the construction of the next two peripheral assemblies. SNL is awaiting the final pressure choice of the Program Review Group before beginning charging activities for the second pressurized, peripheral bundle.

Major equipment purchases including hardware and instrumentation have all been completed. Phase II construction is on schedule to complete by end of April 2012. Pre-Ignition testing will begin in June 2012. The final, destructive ignition test is currently expected to be conducted in July 2012. The quick-look report and data would then be available to OECD partners in August 2012.

This page intentionally blank

5 REFERENCES

1. Lindgren, E.R. and Durbin, S.G., 2007, "Characterization of Thermal-Hydraulic and Ignition Phenomena in Prototypic, Full-Length Boiling Water Reactor Spent Fuel Pool Assemblies after a Complete Loss-of-Coolant Accident," SAND2007-2270.

2. Durbin, S.G. and Lindgren, E.R., 2011, "Sandia Fuel Project Phase I: Pre-Ignition and Ignition Testing of a Commercial 17×17 Pressurized Water Reactor Spent Fuel Assembly under Complete Loss of Coolant Accident Conditions," SAND Report Draft.

3. Durbin, S.G., and Lindgren, E.R. 2008, "Laminar Hydraulic Analysis of a Commercial Pressurized Water Reactor Fuel Assembly," SAND2008-3938.

This page intentionally blank

APPENDIX A – POOL RACK MECHANICAL DRAWINGS

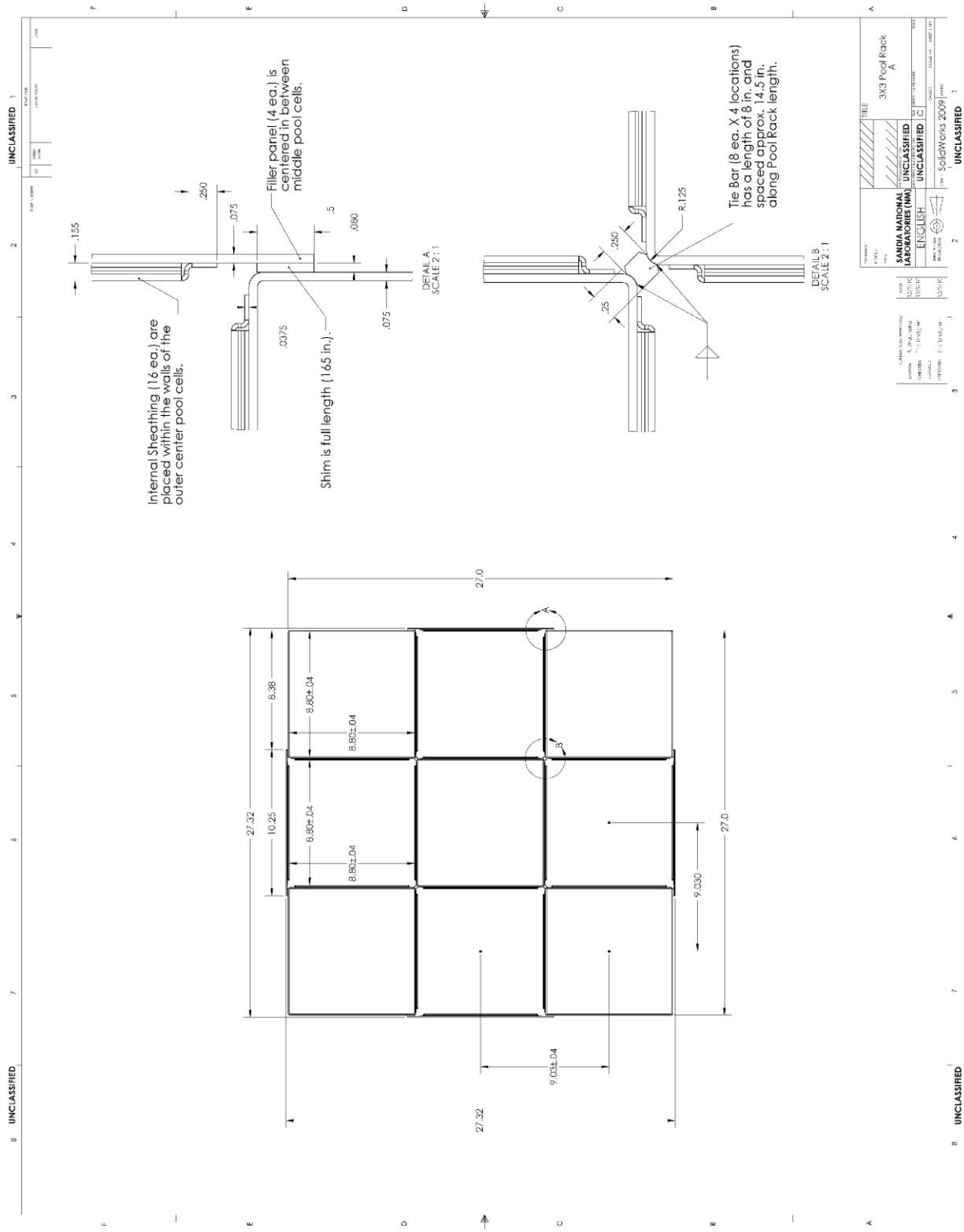

Figure A.1 Pool rack detail drawing – Sheet one.

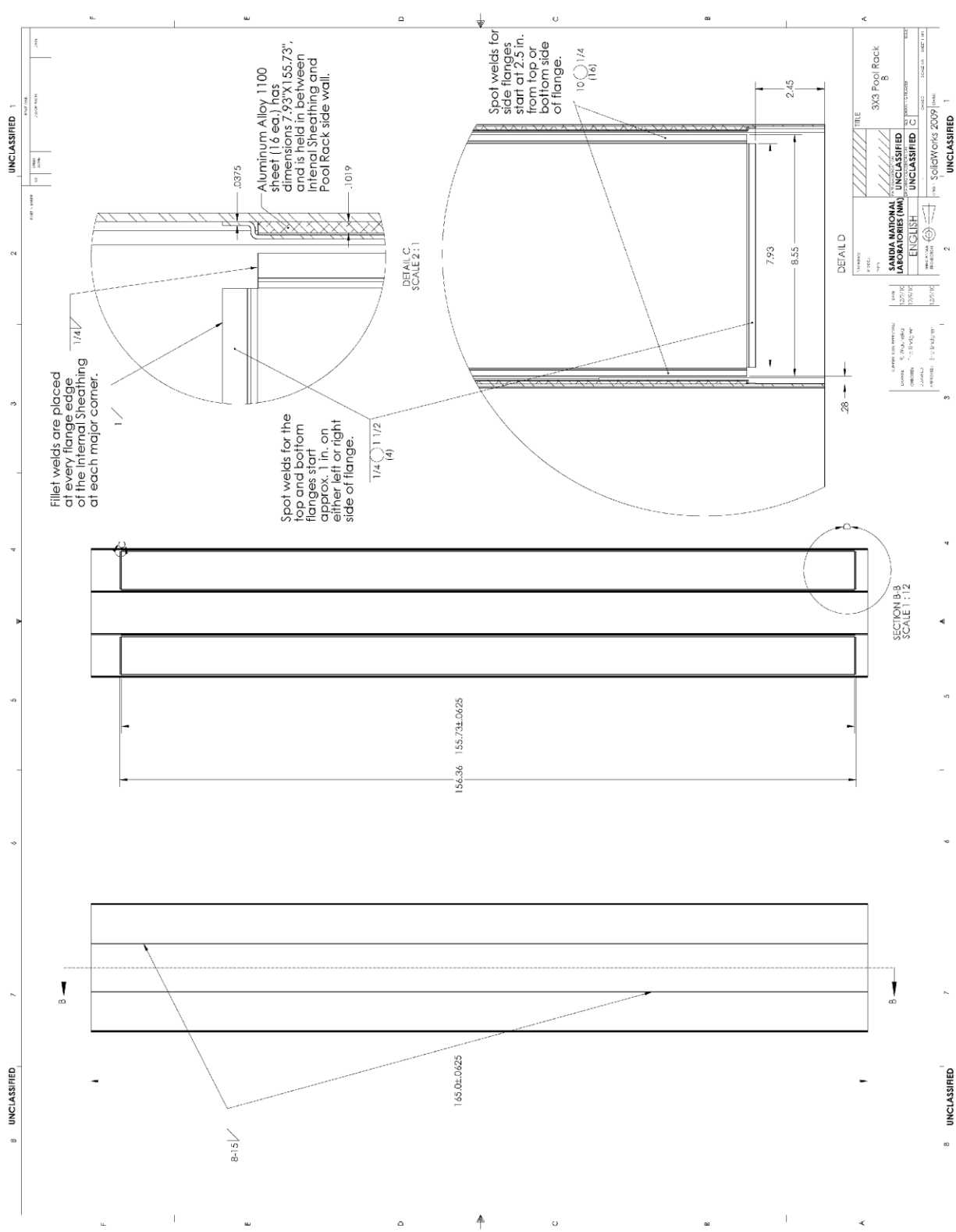

Figure A.2 Pool rack detail drawing – Sheet two.

APPENDIX B – ADDITIONAL GEOMETRIC INFORMATION FOR POROUS MEDIA ANALYSES

The following information is provided for potential use in CFD analyses. The tables define both the blockage and flow areas of the center and peripheral fuel assemblies. The hydraulics are slightly different between the center and peripheral assemblies. In particular, the pool cell area is slightly lower, and the fuel pins are slightly larger. Also, the top of the center assembly is fundamentally different due to the electrical connections and bus plate interfaces.

Table B.1 Definition of flow areas and obstructions in the center, heated assembly.

Segment	Length (m)	*z* (m)	Obstructed Area (m^2)	Rod and GT Cross-Sect. Area (m^2)	Flow Area (m^2)	Porosity based on Pool Cell Area
Top Bus Plates	0.013	4.015	0.0132	0	0.0370	0.737
Short Bundle	0.095	4.003	0.0000	0.0216	0.0286	0.570
Spacer	0.052	3.907	0.0037	0.0216	0.0250	0.497
Long Bundle	0.464	3.855	0.0000	0.0216	0.0286	0.570
Spacer	0.054	3.392	0.0037	0.0216	0.0250	0.497
Short Bundle	0.212	3.338	0.0000	0.0216	0.0286	0.570
IFM	0.042	3.126	0.0037	0.0216	0.0250	0.497
Short Bundle	0.215	3.084	0.0000	0.0216	0.0286	0.570
Spacer	0.053	2.869	0.0037	0.0216	0.0250	0.497
Short Bundle	0.211	2.816	0.0000	0.0216	0.0286	0.570
IFM	0.042	2.606	0.0037	0.0216	0.0250	0.497
Short Bundle	0.217	2.564	0.0000	0.0216	0.0286	0.570
Spacer	0.053	2.347	0.0037	0.0216	0.0250	0.497
Short Bundle	0.212	2.294	0.0000	0.0216	0.0286	0.570
IFM	0.041	2.081	0.0037	0.0216	0.0250	0.497
Short Bundle	0.215	2.041	0.0000	0.0216	0.0286	0.570
Spacer	0.052	1.825	0.0037	0.0216	0.0250	0.497
Long Bundle	0.473	1.773	0.0000	0.0216	0.0286	0.570
Spacer	0.052	1.300	0.0037	0.0216	0.0250	0.497
Long Bundle	0.484	1.248	0.0000	0.0216	0.0286	0.570
Spacer	0.054	0.765	0.0037	0.0216	0.0250	0.497
Long Bundle	0.537	0.711	0.0000	0.0216	0.0286	0.570
Debris Catcher	0.113	0.174	0.0037	0.0216	0.0250	0.497
Bottom Nozzle Plate	0.015	0.061	0.0340	0	0.0162	0.323
Bottom Nozzle Frame	0.025	0.046	0.0054	0	0.0448	0.892
Bottom Nozzle Legs	0.021	0.021	0.0062	0	0.0440	0.876
Base Plate (127 mm ID)	0.013	-0.013	0.0000	0	0.0127	0.252
Inlet Pipe (154 mm ID)	0.914	-0.927	0.0000	0	0.0186	0.371
Pool Cell (224.2 mm)	--	--	--	--	0.0503	1.000

Table B.2 Definition of flow areas and obstructions in the peripheral assemblies.

Segment	Length (m)	z (m)	Obstructed Area (m^2)	Rod and GT Cross-Sect. Area (m^2)	Flow Area (m^2)	Porosity based on Pool Cell Area
Top Nozzle Legs	0.017	4.007	0.0156	0	0.0340	0.685
Top Nozzle Frame	0.003	3.989	0.0040	0	0.0456	0.919
Top Nozzle Plate	0.015	3.986	0.0207	0.0029	0.0259	0.523
Guide Tubes Only	0.034	3.972	0.0000	0.0029	0.0467	0.941
Short Bundle	0.030	3.937	0.0000	0.0217	0.0279	0.562
Spacer	0.052	3.907	0.0037	0.0217	0.0242	0.488
Long Bundle	0.464	3.855	0.0000	0.0217	0.0279	0.562
Spacer	0.054	3.392	0.0037	0.0217	0.0242	0.488
Short Bundle	0.212	3.338	0.0000	0.0217	0.0279	0.562
IFM	0.042	3.126	0.0037	0.0217	0.0242	0.488
Short Bundle	0.215	3.084	0.0000	0.0217	0.0279	0.562
Spacer	0.053	2.869	0.0037	0.0217	0.0242	0.488
Short Bundle	0.211	2.816	0.0000	0.0217	0.0279	0.562
IFM	0.042	2.606	0.0037	0.0217	0.0242	0.488
Short Bundle	0.217	2.564	0.0000	0.0217	0.0279	0.562
Spacer	0.053	2.347	0.0037	0.0217	0.0242	0.488
Short Bundle	0.212	2.294	0.0000	0.0217	0.0279	0.562
IFM	0.041	2.081	0.0037	0.0217	0.0242	0.488
Short Bundle	0.215	2.041	0.0000	0.0217	0.0279	0.562
Spacer	0.052	1.825	0.0037	0.0217	0.0242	0.488
Long Bundle	0.473	1.773	0.0000	0.0217	0.0279	0.562
Spacer	0.052	1.300	0.0037	0.0217	0.0242	0.488
Long Bundle	0.484	1.248	0.0000	0.0217	0.0279	0.562
Spacer	0.054	0.765	0.0037	0.0217	0.0242	0.488
Long Bundle	0.537	0.711	0.0000	0.0217	0.0279	0.562
Debris Catcher	0.113	0.174	0.0037	0.0217	0.0242	0.488
Bottom Nozzle Plate	0.015	0.061	0.0340	0	0.0156	0.314
Bottom Nozzle Frame	0.025	0.046	0.0054	0	0.0442	0.890
Bottom Nozzle Legs	0.021	0.021	0.0062	0	0.0434	0.875
Base Plate (127 mm ID)	0.013	-0.013	0.0000	0	0.0127	0.255
Inlet Pipe (154 mm ID)	0.914	-0.927	0.0000	0	0.0186	0.376
Pool Cell (222.7 mm)	--	--	--	--	0.0496	1.000

DISTRIBUTION

U.S. Nuclear Regulatory Commission (4)
21 Church St.
Washington, DC 20555-0001
Alexander Velazquez, RES, MS C2A07 (2)
Abdelghani Zigh, RES, MS C3A07 (2)

Sandia Internal:

6223	MS0747	Samuel Durbin (2)
6223	MS0747	Eric Lindgren (2)
9532	MS0899	RIM-Reports Management (electronic copy)

This page intentionally blank


Sandia National Laboratories